Generalized Cramer-Rao Bound for Joint Estimation of Target Position and Velocity for Active and Passive Radar Networks

Qian He, *Member, IEEE*, Jianbin Hu, Rick S. Blum, *Fellow, IEEE*, and Yonggang Wu

arXiv:1510.02551v1 [math.ST] 9 Oct 2015

***Abstract*—In this paper, we derive the Cramer-Rao bound (CRB) for joint target position and velocity estimation using an active or passive distributed radar network under more general, and practically occurring, conditions than assumed in previous work. In particular, the presented results allow nonorthogonal signals, spatially dependent Gaussian reflection coefficients, and spatially dependent Gaussian clutter-plus-noise. These bounds allow designers to compare the performance of their developed approaches, which are deemed to be of acceptable complexity, to the best achievable performance. If their developed approaches lead to performance close to the bounds, these developed approaches can be deemed "good enough". A particular recent study where algorithms have been developed for a practical radar application which must involve nonorthognal signals, for which the best performance is unknown, is a great example. The presented results in our paper do not make any assumptions about the approximate location of the target being known from previous target detection signal processing. In addition, for situations in which we do not know some parameters accurately, we also derive the mismatched CRB. Numerical investigations of the mean squared error of the maximum likelihood estimation are employed to support the validity of the CRBs. In order to demonstrate the utility of the provided results to a topic of great current interest, the numerical results focus on a passive radar system using the Global System for Mobile communication (GSM) cellar system.**

***Index Terms*—Distributed networked radar, generalized Cramer-Rao bound (CRB), Global System for Mobile communication (GSM), MIMO radar, parameter estimation, passive radar.**

I. Introduction

The focus of this paper is on new Cramer-Rao bounds (CRB) for estimation of target position and velocity from distributed radar networks, sometimes called MIMO radar systems or multistatic radar systems [1], [2], [3], [4], [5], [6], [7], [8], operating under more general, and practically occurring, conditions than assumed in previous work. In particular, the presented results allow nonorthogonal signals, spatially dependent Gaussian reflection coefficients, and spatially dependent Gaussian clutter-plus-noise, which are cases of great practical interest. In fact, one could argue that all of these conditions are true in any real system. The initial CRBs we present are applicable to both active and passive radar systems, provided the signals of opportunity in the passive systems are assumed to be perfectly estimated from, for example, the direct path reception. These results further assume all the parameters of the observations model are known, including the covariance matrices of the zero-mean Gaussian noise-plus-clutter and reflection coefficients. The mismatched CRB results given in this paper even allow cases where the model assumed by the estimation algorithm is incorrect, including cases where the model for the direct path signal may involve unmodeled noise, interference, or some other imperfection. Similarly, the reflection coefficients, noise, andor interference may be incorrectly modeled and the mistmatched CRB will still provide a lower bound on perfromance.

While both passive and active radar systems are of great interest, passive radar systems may have attracted even greater attention over the past few years due to the tremendous advantages they provide from using existing communication signals to implement a radar, essentially borrowing the already existing transmitter infrastructure and providing no electronic evidence that a radar is operating in a given area. Passive radar, as the name implies, is a radar system which receives only. Instead of actively transmitting signals, it works passively by gathering signals from non-cooperative illuminators of opportunity and reflections from objects in the monitored area to make decisions or provide information about targets. Since transmitters are not required in a passive radar, it has the advantages of low implementation costs, stealth, and the ability to operate in a wide frequency band without concerns of causing interference to existing wireless systems. For these reasons, passive radar systems have attracted the attention of the international radar community. Passive radar systems based on FM [9] and digital illuminators (DAB/DVB-T) [10], or satellite-borne illuminators [11], WIFI [12] and Global System for Mobile communication (GSM) [13] signals have been previously investigated mainly from prototypes or measurements or very simple analytical models. The factors that affect the detection performance of passive coherent location radar systems are discussed in [14]. The ambiguity functions of a set of off-air measurements of signals that may be used for passive coherent location (PCL) radar systems are presented and

The work of Q. He, J. Hu, and Yonggang Wu was supported by the National Nature Science Foundation of China under Grants No. 61102142 and 61371184, the International Science and Technology Cooperation and Exchange Research Program of Sichuan Province under Grant No. 2013HH0006, and the Fundamental Research Funds for the Central Universities under Grant No. ZYGX2013J015. The work of R. S. Blum was supported by the National Science Foundation under Grant No. ECCS-1405579.

Q. He, J. Hu, and Yonggang Wu are with University of Electronic Science and Technology of China, Chengdu, Sichuan 611731 China (emails: qianhe@uestc.edu.cn, 1205858265@qq.com, wyguestc@163.com). R. S. Blum is with Lehigh University, Bethlehem, PA 18015 USA (email: rblum@eecs.lehigh.edu).

analyzed in [15]. The problem of target detection in passive MIMO radar (PMR) networks comprised of non-cooperative transmitters and multichannels is addressed in [16].

As described later, the CRB is a lower bound, in a certain sense, on the covariance matrix of all unbiased estimators. It is a useful tool for evaluating the best possible estimation performance of a radar system. A derivation of the stochastic CRB is provided in [17]. The CRB expressions for the estimation of range (time delay), velocity (Doppler shift) and direction of a point target using an active radar or sonar array are given in [18]. The CRB of DOA estimation of a non-stationary target for a MIMO radar with colocated antennas for a general time division multiplexing (TDM) scheme is computed in [19]. The CRB for bistatic radar channels is derived in [20], which also exploits the relationship between the ambiguity function and the CRB. Cramer-Rao-like bounds for the estimation of a deterministic parameter in the presence of random nuisance parameters are derived in [21], [22].

For the case of multiple transmit and receive antennas employed in a distributed active radar setting, [24] describes the CRB under the assumption of orthogonal signals, spatially independent reflection coefficients, and spatially independent clutter-plus-noise. For estimation of the position and velocity of a single target using a passive radar, the CRB and ambiguity functions are considered in [25] for a multiple transmitter and receiver radar, but only for the case where a single transmitter and receiver pair is selected from among a much larger set of possible pairs. This work does not consider the effect of signal nonorthogonality or spatially dependent reflection coefficients or noise. Under the same assumptions employed in [24], the CRB has been derived for passive radar settings with well estimated signals of opportunity in [26], [27].

Thus, none of the published work has given the CRB for the important and practical case of nonorthogonal signals, spatially dependent reflection coefficients, and spatially dependent noise for joint target position and velocity estimation performance using a distributed passive or active radar network employing all signals available from the multiple transmit and receive antenna paths in an optimum manner. This result is extremely useful since it describes the best achievable performance for some important cases for the first time. Knowing this best achievable performance allows designers to compare the performance of their developed approaches, to these bounds. If their developed approaches lead to performance close to the bounds, these developed approaches can be deemed "good enough" while these developed approaches are typically constrained to have acceptable complexity. The very recent work in [23] provides an excellent example where these results can be extremely useful. In [23], a very practical scenario is considered where a number of transmitters of opportunity send digital TV signals that can not be accurately modeled by assuming the transmitters send a set of nonorthogonal signals. The work in [23] presents an interesting suboptimum algorithm for implementing a radar employing these nonorthogonal signals. However, it is not known how far the performance of the suggested approach in [23] is from the optimum achievable performance. Such information would be extremely useful in judging if the approach suggested in [23] provides a good tradeoff in terms of performance and complexity. Similar questions arise in many related practical applications, some of which involve active radars.

In this paper, we consider these more general cases and derive a generalized CRB and mismatched CRB for joint location and velocity estimation in passive and active distributed radar networks. The presented results do not assume the approximate location of the target is known from previous target detection signal processing, unlike the previous results employing optimum processing using all available antennas [24], [26], [27]. A closed-form Fisher information matrix (FIM) is presented. In a few representative cases, the generalized or mismatched CRB is numerically compared with the mean-squared error (MSE) from maximum likelihood (ML) estimation to show consistency at higher signal-to-noise ratio (SNR). We use GSM signals as illuminators for our numerical passive radar investigations. The rest of this paper is organized as follows. The signal model for active and passive distributed radar networks is presented in Section II. The ML estimate is analyzed in Section II-A. In Section III, the generalized CRB is derived. In Section IV, we derive the mismathed CRB. Performance analysis and numerical examples are presented in Section V. Finally, conclusions are drawn in Section VI.

Throughout this paper, the notation for transpose is $(.)^{\dagger}$, while that for complex conjugate is $(.)^{H}$. The symbol $Diag\{\cdot\}$ denotes a block diagonal matrix with the matrices in the braces being the diagonal blocks, $\mathcal{CN}(\boldsymbol{\mu}, \boldsymbol{R})$ denotes a complex Gaussian distribution with mean vector $\boldsymbol{\mu}$ and covariance matrix $\boldsymbol{R}$, $\mathbb{E}_{\boldsymbol{r}|\boldsymbol{\theta},\boldsymbol{\alpha}}\{\cdot\}$ implies taking expectation with respect to the probability density function (pdf) $p(\boldsymbol{r}|\boldsymbol{\theta}, \boldsymbol{\alpha})$, $\mathrm{Tr}(\cdot)$ denotes the trace of a matrix, $\otimes$ represents the Kronecker product, $\Re(\cdot)$ means taking the real part, $\odot$ represents the Hadamard product, and vec$(\cdot)$ denotes the column vectorizing operator which stacks the columns of a matrix in a column vector.

II. Signal Model

Consider a distributed radar system with M widely spaced single antenna transmit stations and N widely spaced single antenna receive stations, located at (x_m^t, y_m^t), $m = 1, \ldots, M$ and (x_n^r, y_n^r), $n = 1, \ldots, N$ in a two-dimensional Cartesian coordinate system, respectively. The lowpass equivalent time-sampled version of the signal transmitted from the mth transmit station at time instant kT_s is $\sqrt{E_m} s_m(k, \boldsymbol{\alpha_m})$, where T_s is the sampling period, k ($k = 1, \ldots, K$) is an index running over the different time samples, $\boldsymbol{\alpha_m}$ denotes a vector of parameters needed to describe the waveform, and the waveform is normalized using $\sum_{k=1}^{K} |s_m(k, \boldsymbol{\alpha_m})|^2 T_s = 1$. Let E_m denote the energy transmitted by the mth transmit antenna. Then the received waveform at the nth receiver at time kT_s is

$$r_n(k) = \sum_{m=1}^{M} \sqrt{\frac{E_m P_0}{d_{tm}^2 d_{rn}^2}} \zeta_{nm} s_m(kT_s - \tau_{nm}, \boldsymbol{\alpha}_m) e^{j2\pi f_{nm} kT_s} + w_n(k), \tag{1}$$

where τ_{nm}, f_{nm}, and ζ_{nm} represent the time delay, Doppler shift, and reflection coefficient corresponding to the *nm*th path, respectively. The variable d_{tm} denotes the distance between the target and the *m*th transmitter, while d_{rn} denotes the distance between the target and the *n*th receiver. The term $w_n(k)$ denotes clutter-plus-noise at the *n*th receiver at time kT_s. The received signal strength at d_{tm}=d_{rn}=1 is $\sqrt{E_m P_0}$, so P_0 denotes the ratio of received energy at d_{tm}=d_{rn}=1 to transmitted energy. The reflection coefficient ζ_{nm} is assumed to be constant over the observation interval and to have a known complex Gaussian statistical model [28]. Assume the position (x, y) and velocity (v_x, v_y) of the target are deterministic unknowns. The distances d_{tm} and d_{rn} are expressed in terms of (x, y) as

$$d_{tm} = \sqrt{(x_m^t - x)^2 + (y_m^t - y)^2}, \tag{2}$$

$$d_{rn} = \sqrt{(x_n^r - x)^2 + (y_n^r - y)^2}. \tag{3}$$

The time delay τ_{nm} is also a function of the unknown target position (x, y)

$$\begin{aligned}\tau_{nm} &= \frac{\sqrt{(x_m^t - x)^2 + (y_m^t - y)^2} + \sqrt{(x_n^r - x)^2 + (y_n^r - y)^2}}{c} \\ &= \frac{d_{tm} + d_{rn}}{c},\end{aligned} \tag{4}$$

where c denotes the speed of light, The Doppler shift f_{nm} is a function of the unknown target position (x, y) and velocity (v_x, v_y) given by

$$f_{nm} = \frac{v_x (x_m^t - x) + v_y (y_m^t - y)}{\lambda d_{tm}} + \frac{v_x (x_n^r - x) + v_y (y_n^r - y)}{\lambda d_{rn}}, \tag{5}$$

where λ denotes the wavelength. Define an unknown parameter vector $\boldsymbol{\theta}$ that collects the parameters to be estimated

$$\boldsymbol{\theta} = \left[x, y, v_x, v_y\right]^\dagger. \tag{6}$$

The observations from the *n*th receiver can be expressed as

$$\begin{aligned}\boldsymbol{r}_n &= [r_n(1), r_n(2), \cdots, r_n(K)]^\dagger &(7)\\ &= \boldsymbol{U}_n \boldsymbol{\zeta}_n + \boldsymbol{w}_n, &(8)\end{aligned}$$

where $\boldsymbol{U}_n$ is a $K \times M$ matrix that collects the time delayed and Doppler shifted signals at the *n*th receiver as

$$\boldsymbol{U}_n = [\boldsymbol{u}_n(1), \boldsymbol{u}_n(2), \ldots, \boldsymbol{u}_n(K)]^\dagger, \tag{9}$$

where

$$\boldsymbol{u}_n(k) = [u_{n1}(k), u_{n2}(k), \cdots, u_{nM}(k)]^\dagger, \tag{10}$$

and

$$u_{nm}(k) = \sqrt{\frac{E_m P_0}{d_{tm}^2 d_{rn}^2}} s_m(kT_s - \tau_{nm}, \boldsymbol{\alpha_m}) e^{j2\pi f_{nm} k T_s}. \tag{11}$$

The $M \times 1$ reflection coefficient vector $\boldsymbol{\zeta}_n$ can be expressed as $\boldsymbol{\zeta}_n = [\zeta_{n1}, \cdots, \zeta_{nM}]^\dagger$. Denote the vector of noise samples at the *n*th receiver as $\boldsymbol{w}_n = [w_n(1), \cdots, w_n(K)]^\dagger$. The observations from the set of all receivers can be written as

$$\begin{aligned}\boldsymbol{r} &= \left[\boldsymbol{r}_1^\dagger, \boldsymbol{r}_2^\dagger, \cdots, \boldsymbol{r}_N^\dagger\right]^\dagger \\ &= \boldsymbol{S}\boldsymbol{\zeta} + \boldsymbol{w},\end{aligned} \tag{12}$$

where $\boldsymbol{S}$ collects the time delayed and Doppler shifted signals from all paths

$$\boldsymbol{S} = Diag\{\boldsymbol{U}_1, \boldsymbol{U}_2, \ldots, \boldsymbol{U}_N\}. \tag{13}$$

The $\boldsymbol{\zeta}$ in (12) collects reflection coefficients for all paths

$$\boldsymbol{\zeta} = \left[\boldsymbol{\zeta}_1^\dagger, \cdots, \boldsymbol{\zeta}_N^\dagger\right]^\dagger, \tag{14}$$

and it is assumed that $\boldsymbol{\zeta}$ is a complex Gaussian distributed vector with zero mean and covariance matrix $\boldsymbol{R} = \mathbb{E}\{\boldsymbol{\zeta}\boldsymbol{\zeta}^H\}$, i.e. $\boldsymbol{\zeta} \sim \mathcal{CN}(\boldsymbol{0}, \boldsymbol{R})$. The $\boldsymbol{w}$ in (12) denotes the clutter-plus-noise vector

$$\boldsymbol{w} = \left[\boldsymbol{w}_1^\dagger, \cdots, \boldsymbol{w}_N^\dagger\right]^\dagger, \tag{15}$$

which is assumed to be complex Gaussian distributed with zero mean and covariance matrix $\boldsymbol{Q} = \mathbb{E}\{\boldsymbol{w}\boldsymbol{w}^H\}$, i.e., $\boldsymbol{w} \sim \mathcal{CN}(\boldsymbol{0}, \boldsymbol{Q})$. Assume that the noise vector $\boldsymbol{w}$ is independent from the reflection coefficient vector $\boldsymbol{\zeta}$.

A. Maximum Likelihood Estimation

In this and the next section (Sections II and III), we assume $\boldsymbol{S}$ (and thus $\boldsymbol{\alpha}$), $\boldsymbol{Q}$, and $\boldsymbol{R}$ are known to the estimation algorithm. We address other cases later. Using the signal model in (12) and the fact that the linear combination of two Gaussian vectors is also Gaussian, the likelihood function conditioned on the waveform parameter vector

$$\boldsymbol{\alpha} = [\boldsymbol{\alpha_1}, \ldots, \boldsymbol{\alpha}_M]^\dagger, \tag{16}$$

can be obtained as

$$p(\boldsymbol{r}|\boldsymbol{\theta}, \boldsymbol{\alpha}) = \frac{1}{\pi^{KN} \det(\boldsymbol{C})} \exp(-\boldsymbol{r}^H \boldsymbol{C}^{-1} \boldsymbol{r}), \tag{17}$$

where $\boldsymbol{C}$ denotes the covariance matrix

$$\begin{aligned}\boldsymbol{C} &= \mathbb{E}\left\{(\boldsymbol{S}\boldsymbol{\zeta} + \boldsymbol{w})(\boldsymbol{S}\boldsymbol{\zeta} + \boldsymbol{w})^H\right\} \\ &= \mathbb{E}\left\{\boldsymbol{S}\boldsymbol{\zeta}\boldsymbol{\zeta}^H \boldsymbol{S}^H + \boldsymbol{w}\boldsymbol{w}^H\right\} \\ &= \boldsymbol{S}\boldsymbol{R}\boldsymbol{S}^H + \boldsymbol{Q}.\end{aligned} \tag{18}$$

The log-likelihood function can be written as

$$\begin{aligned}L(\boldsymbol{r}|\boldsymbol{\theta}, \boldsymbol{\alpha}) &= \ln p(\boldsymbol{r}|\boldsymbol{\theta}, \boldsymbol{\alpha}) \\ &= -\boldsymbol{r}^H \boldsymbol{C}^{-1} \boldsymbol{r} - \ln(\det(\boldsymbol{C})) - KN \ln(\pi).\end{aligned} \tag{19}$$

Neglecting the last constant term of the second line in (19) and assuming known or perfectly estimated $\boldsymbol{\alpha}$, the (ML) estimate of the unknown parameter vector $\boldsymbol{\theta}$ can be calculated as

$$\begin{aligned}\hat{\boldsymbol{\theta}}_{ML} &= \arg\max_{\boldsymbol{\theta}} L(\boldsymbol{r}|\boldsymbol{\theta}, \boldsymbol{\alpha}) \\ &= \arg\max_{\boldsymbol{\theta}} \left\{-\boldsymbol{r}^H \boldsymbol{C}^{-1} \boldsymbol{r} - \ln(\det(\boldsymbol{C}))\right\}.\end{aligned} \tag{20}$$

III. Generalized Cramer-Rao Bound

In this section, we provide the CRB for jointly estimating the target location (x,y) and velocity $\left(v_x, v_y\right)$ for the case where $\boldsymbol{S}$ (and thus $\boldsymbol{\alpha}$), $\boldsymbol{Q}$, and $\boldsymbol{R}$ are known to the estimation algorithm. The first step in obtaining the CRB is to compute the FIM, which is a 4×4 matrix related to the second order derivatives of the log-likelihood function

$$\boldsymbol{J}\left(\boldsymbol{\theta}|\boldsymbol{\alpha}\right)=\mathbb{E}_{\boldsymbol{r}|\boldsymbol{\theta},\boldsymbol{\alpha}}\left\{\nabla_{\boldsymbol{\theta}}L\left(\boldsymbol{r}|\boldsymbol{\theta},\boldsymbol{\alpha}\right)\left[\nabla_{\boldsymbol{\theta}}L\left(\boldsymbol{r}|\boldsymbol{\theta},\boldsymbol{\alpha}\right)\right]^{\dagger}\right\}. \tag{21}$$

Considering the likelihood is a function of τ_{nm}, f_{nm}, d_{tm}, and d_{rn} $(n=1,\cdots,N,\ m=1,\cdots,M)$, which depend on $\boldsymbol{\theta}=\left[x,y,v_x,v_y\right]^{\dagger}$, we define an intermediate parameter vector

$$\begin{aligned}\boldsymbol{\vartheta}=&[\boldsymbol{\tau}^{\dagger},\boldsymbol{f}^{\dagger},\boldsymbol{d}_t^{\dagger},\boldsymbol{d}_r^{\dagger}]^{\dagger}\\ =&[\tau_{11},\tau_{12},\cdots,\tau_{NM},f_{11},f_{12},\cdots,f_{NM},\\ &d_{t1},d_{t2},\cdots,d_{tM},d_{r1},d_{r2},\cdots d_{rN}]^{\dagger}\end{aligned} \tag{22}$$

where $\boldsymbol{\tau}=[\tau_{11},\tau_{12},\cdots,\tau_{NM}]^{\dagger}$, $\boldsymbol{f}=[f_{11},f_{12},\cdots,f_{NM}]^{\dagger}$, $\boldsymbol{d_t}=[d_{t1},d_{t2},\cdots,d_{tM}]^{\dagger}$ and $\boldsymbol{d_r}=[d_{r1},d_{r2},\cdots,d_{rN}]^{\dagger}$ collect the unknown time delays, Doppler shifts, and distance parameters, respectively. According to the chain rule, the FIM can be derived by

$$\boldsymbol{J}\left(\boldsymbol{\theta}|\boldsymbol{\alpha}\right)=\left(\nabla_{\boldsymbol{\theta}}\boldsymbol{\vartheta}^{\dagger}\right)\boldsymbol{J}\left(\boldsymbol{\vartheta}|\boldsymbol{\alpha}\right)\left(\nabla_{\boldsymbol{\theta}}\boldsymbol{\vartheta}^{\dagger}\right)^{\dagger}, \tag{23}$$

where $\boldsymbol{J}\left(\boldsymbol{\vartheta}|\boldsymbol{\alpha}\right)=\mathbb{E}_{\boldsymbol{r}|\boldsymbol{\vartheta},\boldsymbol{\alpha}}\left\{\nabla_{\boldsymbol{\vartheta}}L\left(\boldsymbol{r}|\boldsymbol{\vartheta},\boldsymbol{\alpha}\right)\left[\nabla_{\boldsymbol{\vartheta}}L\left(\boldsymbol{r}|\boldsymbol{\vartheta},\boldsymbol{\alpha}\right)\right]^{\dagger}\right\}$.

A. Calculation of $\nabla_{\boldsymbol{\theta}}\boldsymbol{\vartheta}^{\dagger}$

Recalling (6) and (22), we have

$$\nabla_{\boldsymbol{\theta}}\boldsymbol{\vartheta}^{\dagger}=\begin{bmatrix}\boldsymbol{F} & \boldsymbol{G} & \boldsymbol{D}_t & \boldsymbol{D}_r\\ \boldsymbol{0} & \boldsymbol{H} & \boldsymbol{0} & \boldsymbol{0}\end{bmatrix}, \tag{24}$$

where

$$\boldsymbol{F}=\begin{bmatrix}\frac{\partial\tau_{11}}{\partial x} & \frac{\partial\tau_{12}}{\partial x} & \cdots & \frac{\partial\tau_{NM}}{\partial x}\\ \frac{\partial\tau_{11}}{\partial y} & \frac{\partial\tau_{12}}{\partial y} & \cdots & \frac{\partial\tau_{NM}}{\partial y}\end{bmatrix}, \tag{25}$$

$$\boldsymbol{G}=\begin{bmatrix}\frac{\partial f_{11}}{\partial x} & \frac{\partial f_{12}}{\partial x} & \cdots & \frac{\partial f_{NM}}{\partial x}\\ \frac{\partial f_{11}}{\partial y} & \frac{\partial f_{12}}{\partial y} & \cdots & \frac{\partial f_{NM}}{\partial y}\end{bmatrix}, \tag{26}$$

$$\boldsymbol{H}=\begin{bmatrix}\frac{\partial f_{11}}{\partial v_x} & \frac{\partial f_{12}}{\partial v_x} & \cdots & \frac{\partial f_{NM}}{\partial v_x}\\ \frac{\partial f_{11}}{\partial v_y} & \frac{\partial f_{12}}{\partial v_y} & \cdots & \frac{\partial f_{NM}}{\partial v_y}\end{bmatrix}, \tag{27}$$

$$\boldsymbol{D}_t=\begin{bmatrix}\frac{\partial d_{t1}}{\partial x} & \frac{\partial d_{t2}}{\partial x} & \cdots & \frac{\partial d_{tM}}{\partial x}\\ \frac{\partial d_{t1}}{\partial y} & \frac{\partial d_{t2}}{\partial y} & \cdots & \frac{\partial d_{tM}}{\partial y},\end{bmatrix}, \tag{28}$$

and

$$\boldsymbol{D}_r=\begin{bmatrix}\frac{\partial d_{r1}}{\partial x} & \frac{\partial d_{r2}}{\partial x} & \cdots & \frac{\partial d_{rN}}{\partial x}\\ \frac{\partial d_{r1}}{\partial y} & \frac{\partial d_{r2}}{\partial y} & \cdots & \frac{\partial d_{rN}}{\partial y}\end{bmatrix}. \tag{29}$$

Using calculations drawing on (2)-(5), the elements of the matrices in (25)-(29) will be described as

$$a_{nm}=\frac{\partial\tau_{nm}}{\partial x}=\frac{1}{c}\left(\frac{x-x_m^t}{d_{tm}}+\frac{x-x_n^r}{d_{rn}}\right), \tag{30}$$

$$b_{nm}=\frac{\partial\tau_{nm}}{\partial y}=\frac{1}{c}\left(\frac{y-y_m^t}{d_{tm}}+\frac{y-y_n^r}{d_{rn}}\right), \tag{31}$$

$$\begin{aligned}e_{nm}=&\frac{\partial f_{nm}}{\partial x}=-\frac{v_x}{\lambda}\left(\frac{1}{d_{tm}}+\frac{1}{d_{rn}}\right)\\ &+\frac{\left(x_m^t-x\right)}{\lambda\left(d_{tm}\right)^3}\left[v_x\left(x_m^t-x\right)+v_y\left(y_m^t-y\right)\right]\\ &+\frac{\left(x_n^r-x\right)}{\lambda\left(d_{rn}\right)^3}\left[v_x\left(x_n^r-x\right)+v_y\left(y_n^r-y\right)\right],\end{aligned} \tag{32}$$

$$\begin{aligned}g_{nm}=&\frac{\partial f_{nm}}{\partial y}=-\frac{v_y}{\lambda}\left(\frac{1}{d_{tm}}+\frac{1}{d_{rn}}\right)\\ &+\frac{\left(y_m^t-y\right)}{\lambda\left(d_{tm}\right)^3}\left[v_x\left(x_m^t-x\right)+v_y\left(y_m^t-y\right)\right]\\ &+\frac{\left(y_n^r-y\right)}{\lambda\left(d_{rn}\right)^3}\left[v_x\left(x_n^r-x\right)+v_y\left(y_n^r-y\right)\right],\end{aligned} \tag{33}$$

$$\beta_{nm}=\frac{\partial f_{nm}}{\partial v_x}=\frac{x_m^t-x}{\lambda d_{tm}}+\frac{x_n^r-x}{\lambda d_{rn}}, \tag{34}$$

$$\kappa_{nm}=\frac{\partial f_{nm}}{\partial v_y}=\frac{y_m^t-y}{\lambda d_{tm}}+\frac{y_n^r-y}{\lambda d_{rn}}, \tag{35}$$

$$\upsilon_{tm}=\frac{\partial d_{tm}}{\partial x}=\frac{x-x_m^t}{d_{tm}}, \tag{36}$$

$$l_{tm}=\frac{\partial d_{tm}}{\partial y}=\frac{y-y_m^t}{d_{tm}}, \tag{37}$$

$$\eta_{rn}=\frac{\partial d_{rn}}{\partial x}=\frac{x-x_n^r}{d_{rn}}, \tag{38}$$

and

$$\psi_{rn}=\frac{\partial d_{rn}}{\partial y}=\frac{y-y_n^r}{d_{rn}}. \tag{39}$$

Note that a_{nm}, b_{nm}, e_{nm}, g_{nm}, β_{nm}, κ_{nm}, υ_{tm}, l_{tm}, η_{rn} and ψ_{rn} are determined by the target position and velocity, as well as the position of the receivers and transmitters.

B. Calculation of $\boldsymbol{J}(\boldsymbol{\vartheta}|\boldsymbol{\alpha})$

According to the likelihood function in (19), the ijth element of the FIM for the parameter vector $\boldsymbol{\vartheta}$ is given by [29]

$$\left[\boldsymbol{J}(\boldsymbol{\vartheta}|\boldsymbol{\alpha})\right]_{ij}=\mathrm{Tr}\left(\boldsymbol{C}^{-1}\frac{\partial\boldsymbol{C}}{\partial\vartheta_i}\boldsymbol{C}^{-1}\frac{\partial\boldsymbol{C}}{\partial\vartheta_j}\right). \tag{40}$$

Using the following identities, [30]

$$\mathrm{Tr}\left(\boldsymbol{ABXY}\right)=\left(\mathrm{vec}\left(\boldsymbol{Y}^{\dagger}\right)\right)^{\dagger}\left(\boldsymbol{X}^{\dagger}\otimes\boldsymbol{A}\right)\mathrm{vec}\left(\boldsymbol{B}\right) \tag{41}$$

and

$$\mathrm{Tr}\left(\boldsymbol{AB}\right)=\mathrm{Tr}\left(\boldsymbol{BA}\right), \tag{42}$$

we can rewrite (40) as

$$\begin{aligned}\left[\boldsymbol{J}\left(\boldsymbol{\vartheta}|\boldsymbol{\alpha}\right)\right]_{ij}=&Tr\left(\frac{\partial\boldsymbol{C}}{\partial\vartheta_i}\boldsymbol{C}^{-1}\frac{\partial\boldsymbol{C}}{\partial\vartheta_j}\boldsymbol{C}^{-1}\right)\\ =&\left(\frac{\partial\boldsymbol{C}_{vec}}{\partial\vartheta_i}\right)^{H}\left(\boldsymbol{C}^{-\dagger}\otimes\boldsymbol{C}^{-1}\right)\left(\frac{\partial\boldsymbol{C}_{vec}}{\partial\vartheta_j}\right),\end{aligned} \tag{43}$$

where $\boldsymbol{C}_{vec} = \mathrm{vec}(\boldsymbol{C})$. Calculation of the derivatives and further simplification of (43) are provided in Appendix A. Then we can get the final equation

$$\boldsymbol{J}(\boldsymbol{\theta}|\boldsymbol{\alpha}) = \sum_{p=1}^{N}\sum_{q=1}^{M}\sum_{n=1}^{N}\sum_{m=1}^{M}\begin{bmatrix} A_{11} & A_{12} & A_{13} & A_{14} \\ A_{21} & A_{22} & A_{23} & A_{24} \\ A_{31} & A_{32} & A_{33} & A_{34} \\ A_{41} & A_{42} & A_{43} & A_{44} \end{bmatrix}, \quad (44)$$

where

$$\begin{aligned}\boldsymbol{A}_{11} = {} & a_{pq}(a_{nm}(\boldsymbol{J}_{\boldsymbol{\tau\tau}})_{c,d} + e_{nm}(\boldsymbol{J}_{\boldsymbol{f\tau}})_{c,d} + \\ & \upsilon_{tm}(\boldsymbol{J}_{\boldsymbol{d_t\tau}})_{m,d}/N + \eta_{rn}(\boldsymbol{J}_{\boldsymbol{d_r\tau}})_{n,d}/M) \\ & + e_{pq}(a_{nm}(\boldsymbol{J}_{\boldsymbol{\tau f}})_{c,d} + e_{nm}(\boldsymbol{J}_{\boldsymbol{ff}})_{c,d} + \\ & \upsilon_{tm}(\boldsymbol{J}_{\boldsymbol{d_tf}})_{m,d}/N + \eta_{rn}(\boldsymbol{J}_{\boldsymbol{d_rf}})_{n,d}/M) \\ & + \upsilon_{tq}/N(a_{nm}(\boldsymbol{J}_{\boldsymbol{\tau d_t}})_{c,q} + e_{nm}(\boldsymbol{J}_{\boldsymbol{fd_t}})_{c,q} + \\ & \upsilon_{tm}(\boldsymbol{J}_{\boldsymbol{d_td_t}})_{m,q}/N + \eta_{rn}(\boldsymbol{J}_{\boldsymbol{d_rd_t}})_{n,q}/M) \\ & + \eta_{rp}/M(a_{nm}(\boldsymbol{J}_{\boldsymbol{\tau d_r}})_{c,p} + e_{nm}(\boldsymbol{J}_{\boldsymbol{fd_r}})_{c,p} + \\ & \upsilon_{tm}(\boldsymbol{J}_{\boldsymbol{d_td_r}})_{m,p}/N + \eta_{rn}(\boldsymbol{J}_{\boldsymbol{d_rd_r}})_{n,p}/M), \end{aligned} \quad (45)$$

$$\begin{aligned}\boldsymbol{A}_{12} = \boldsymbol{A}_{21} = {} & b_{pq}(a_{nm}(\boldsymbol{J}_{\boldsymbol{\tau\tau}})_{c,d} + e_{nm}(\boldsymbol{J}_{\boldsymbol{f\tau}})_{c,d} + \\ & \upsilon_{tm}(\boldsymbol{J}_{\boldsymbol{d_t\tau}})_{m,d}/N + \eta_{rn}(\boldsymbol{J}_{\boldsymbol{d_r\tau}})_{n,d}/M) \\ & + g_{pq}(a_{nm}(\boldsymbol{J}_{\boldsymbol{\tau f}})_{c,d} + e_{nm}(\boldsymbol{J}_{\boldsymbol{ff}})_{c,d} + \\ & \upsilon_{tm}(\boldsymbol{J}_{\boldsymbol{d_tf}})_{m,d}/N + \eta_{rn}(\boldsymbol{J}_{\boldsymbol{d_rf}})_{n,d}/M) \\ & + l_{tq}/N(a_{nm}(\boldsymbol{J}_{\boldsymbol{\tau d_t}})_{c,q} + e_{nm}(\boldsymbol{J}_{\boldsymbol{fd_t}})_{c,q} + \\ & \upsilon_{tm}(\boldsymbol{J}_{\boldsymbol{d_td_t}})_{m,q}/N + \eta_{rn}(\boldsymbol{J}_{\boldsymbol{d_rd_t}})_{n,q}/M) \\ & + \psi_{rp}/M(a_{nm}(\boldsymbol{J}_{\boldsymbol{\tau d_r}})_{c,p} + e_{nm}(\boldsymbol{J}_{\boldsymbol{fd_r}})_{c,p} + \\ & \upsilon_{tm}(\boldsymbol{J}_{\boldsymbol{d_td_r}})_{m,p}/N + \eta_{rn}(\boldsymbol{J}_{\boldsymbol{d_rd_r}})_{n,p}/M), \end{aligned} \quad (46)$$

$$\begin{aligned}A_{13} = A_{31} = {} & \beta_{pq}[a_{nm}(\boldsymbol{J}_{\boldsymbol{\tau f}})_{c,d} + e_{nm}(\boldsymbol{J}_{\boldsymbol{ff}})_{c,d} + \\ & \upsilon_{tm}(\boldsymbol{J}_{\boldsymbol{d_tf}})_{m,d}/N + \eta_{rn}(\boldsymbol{J}_{\boldsymbol{d_rf}})_{n,d}/M], \end{aligned} \quad (47)$$

$$\begin{aligned}A_{14} = A_{41} = {} & k_{pq}[a_{nm}(\boldsymbol{J}_{\boldsymbol{\tau f}})_{c,d} + e_{nm}(\boldsymbol{J}_{\boldsymbol{ff}})_{c,d} + \\ & \upsilon_{tm}(\boldsymbol{J}_{\boldsymbol{d_tf}})_{m,d}/N + \eta_{rn}(\boldsymbol{J}_{\boldsymbol{d_rf}})_{n,d}/M], \end{aligned} \quad (48)$$

$$\begin{aligned}A_{22} = {} & b_{pq}(b_{nm}(\boldsymbol{J}_{\boldsymbol{\tau\tau}})_{c,d} + g_{nm}(\boldsymbol{J}_{\boldsymbol{f\tau}})_{c,d} + \\ & l_{tm}(\boldsymbol{J}_{\boldsymbol{d_t\tau}})_{m,d}/N + \psi_{rn}(\boldsymbol{J}_{\boldsymbol{d_r\tau}})_{n,d}/M) \\ & + g_{pq}(b_{nm}(\boldsymbol{J}_{\boldsymbol{\tau f}})_{c,d} + g_{nm}(\boldsymbol{J}_{\boldsymbol{ff}})_{c,d} + \\ & l_{tm}(\boldsymbol{J}_{\boldsymbol{d_tf}})_{m,d}/N + \psi_{rn}(\boldsymbol{J}_{\boldsymbol{d_rf}})_{n,d}/M) \\ & + l_{tq}/N(b_{nm}(\boldsymbol{J}_{\boldsymbol{\tau d_t}})_{c,q} + g_{nm}(\boldsymbol{J}_{\boldsymbol{fd_t}})_{c,q} + \\ & l_{tm}(\boldsymbol{J}_{\boldsymbol{d_td_t}})_{m,q}/N + \psi_{rn}(\boldsymbol{J}_{\boldsymbol{d_rd_t}})_{n,q}/M) \\ & + \psi_{rp}/M(b_{nm}(\boldsymbol{J}_{\boldsymbol{\tau d_r}})_{c,p} + g_{nm}(\boldsymbol{J}_{\boldsymbol{fd_r}})_{c,p} + \\ & l_{tm}(\boldsymbol{J}_{\boldsymbol{d_td_r}})_{m,p}/N + \psi_{rn}(\boldsymbol{J}_{\boldsymbol{d_rd_r}})_{n,p}/M) \end{aligned} \quad (49)$$

$$\begin{aligned}A_{23} = A_{32} = {} & \beta_{pq}[b_{nm}(\boldsymbol{J}_{\boldsymbol{\tau f}})_{c,d} + g_{nm}(\boldsymbol{J}_{\boldsymbol{ff}})_{c,d} + \\ & l_{tm}(\boldsymbol{J}_{\boldsymbol{d_tf}})_{m,d}/N + \psi_{rn}(\boldsymbol{J}_{\boldsymbol{d_rf}})_{n,d}/M], \end{aligned} \quad (50)$$

$$\begin{aligned}A_{24} = A_{42} = {} & k_{pq}[b_{nm}(\boldsymbol{J}_{\boldsymbol{\tau f}})_{c,d} + g_{nm}(\boldsymbol{J}_{\boldsymbol{ff}})_{c,d} + \\ & l_{tm}(\boldsymbol{J}_{\boldsymbol{d_tf}})_{m,d}/N + \psi_{rn}(\boldsymbol{J}_{\boldsymbol{d_rf}})_{n,d}/M], \end{aligned} \quad (51)$$

$$A_{33} = \beta_{pq}\beta_{nm}(\boldsymbol{J}_{\boldsymbol{ff}})_{c,d}, \quad (52)$$

$$A_{34} = A_{43} = k_{pq}\beta_{nm}(\boldsymbol{J}_{\boldsymbol{ff}})_{c,d}, \quad (53)$$

and

$$A_{44} = k_{pq}k_{nm}(\boldsymbol{J}_{\boldsymbol{ff}})_{c,d}, \quad (54)$$

where $c = M(n-1)+m$ and $d = M(p-1)+q$. $\boldsymbol{J}_{\boldsymbol{\tau\tau}}$, $\boldsymbol{J}_{\boldsymbol{\tau f}}$, $\boldsymbol{J}_{\boldsymbol{f\tau}}$, $\boldsymbol{J}_{\boldsymbol{\tau d_t}}$, $\boldsymbol{J}_{\boldsymbol{d_t\tau}}$, $\boldsymbol{J}_{\boldsymbol{\tau d_r}}$, $\boldsymbol{J}_{\boldsymbol{d_r\tau}}$, $\boldsymbol{J}_{\boldsymbol{ff}}$, $\boldsymbol{J}_{\boldsymbol{fd_t}}$, $\boldsymbol{J}_{\boldsymbol{d_tf}}$, $\boldsymbol{J}_{\boldsymbol{fd_r}}$, $\boldsymbol{J}_{\boldsymbol{d_rf}}$, $\boldsymbol{J}_{\boldsymbol{d_td_t}}$, $\boldsymbol{J}_{\boldsymbol{d_td_r}}$, $\boldsymbol{J}_{\boldsymbol{d_rd_t}}$, $\boldsymbol{J}_{\boldsymbol{d_rd_r}}$ are defined in (72). It should be noted that, the results obtained here, say (44)-(54), are a highly nontrival extension of the previous results in [24]. Unfortunately, they are, as one might expect, considerably more complicated but they describe the best possible estimation performance in non-ideal scenarios that are of great practical interest in the following sense. Given any unbiased estimator $\hat{\boldsymbol{\theta}}$ of an unknown parameter $\boldsymbol{\theta}$ based on an observation vector $\boldsymbol{r}$, when $\boldsymbol{\alpha}$ is assumed known and fixed, we have [29]

$$\mathrm{MSE} = \mathbb{E}_{\boldsymbol{r}|\boldsymbol{\theta},\boldsymbol{\alpha}}\left\{(\hat{\boldsymbol{\theta}}-\boldsymbol{\theta})(\hat{\boldsymbol{\theta}}-\boldsymbol{\theta})^{\dagger}\right\} \geq \mathrm{CRB}(\boldsymbol{\theta}|\boldsymbol{\alpha}) = \boldsymbol{J}^{-1}(\boldsymbol{\theta}|\boldsymbol{\alpha}). \quad (55)$$

which is the standard CRB for vector parameters where $\boldsymbol{A} \geq \boldsymbol{B}$ means $\boldsymbol{A}-\boldsymbol{B}$ is positive semidefinite, and MSE is the mean squared error matrix of the unbiased estimator.

IV. Cramer-Rao Bound For Mismatched Case

In order to find an ML estimate or use the CRB result in (55), now called the generalized CRB (GCRB), we must know the actual values of the signal matrix $\boldsymbol{S}$ (and thus $\boldsymbol{\alpha}$) from (13), the reflection coefficients covariance matrix $\boldsymbol{R}$ described near (14), and the noise covariance matrix $\boldsymbol{Q}$ described near (15). Here, we assume the estimation algorithm employs incorrect values for these matrices denoted by $\boldsymbol{S}_0$, $\boldsymbol{R}_0$, and $\boldsymbol{Q}_0$ respectively. The incorrect values $\boldsymbol{S}_0$, $\boldsymbol{R}_0$, and $\boldsymbol{Q}_0$ might be obtained from some inaccurate estimation. Given the estimation algorithm uses these incorrect values $\boldsymbol{S}_0$, $\boldsymbol{R}_0$, and $\boldsymbol{Q}_0$, we find a lower bound on the estimation performance using some recently published work [31]. In the case described, the assumed likelihood function is

$$p_0(\boldsymbol{r}|\boldsymbol{\theta},\boldsymbol{\alpha}) = \frac{1}{\pi^{KN}\det\boldsymbol{C_0}}\exp(-\boldsymbol{r}^H\boldsymbol{C_0}^{-1}\boldsymbol{r}), \quad (56)$$

where $\boldsymbol{C}_0 = \boldsymbol{S}_0\boldsymbol{R}_0\boldsymbol{S}_0{}^H + \boldsymbol{Q}_0$. To avoid confusion with the GCRB, we denote the actual values of the signal matrix from (13), the reflection coefficients covariance matrix described near (14), and noise covariance matrix described near (15) by $\boldsymbol{S}_1$, $\boldsymbol{R}_1$, and $\boldsymbol{Q}_1$.

Thus, the actual likelihood function is

$$p_1(\boldsymbol{r}|\boldsymbol{\theta},\boldsymbol{\alpha}) = \frac{1}{\pi^{KN}\det\boldsymbol{C}_1}\exp(-\boldsymbol{r}^H\boldsymbol{C}_1{}^{-1}\boldsymbol{r}) \quad (57)$$

where $\boldsymbol{C}_1 = \boldsymbol{S}_1\boldsymbol{R}_1\boldsymbol{S}_1{}^H + \boldsymbol{Q}_1$. According to [31], we know that

$$\mathrm{MSE}_{mis} \geq \mathrm{CRB}_{mis}(\boldsymbol{\theta}|\boldsymbol{\alpha}) = \boldsymbol{J}_{\boldsymbol{mis}}{}^{-1}(\boldsymbol{\theta}|\boldsymbol{\alpha}). \quad (58)$$

where $\mathrm{MSE}_{\mathrm{mis}}$, $\mathrm{CRB}_{\mathrm{mis}}(\boldsymbol{\theta}|\boldsymbol{\alpha})$ and $\boldsymbol{J}_{\boldsymbol{mis}}(\boldsymbol{\theta}|\boldsymbol{\alpha})$ denote the MSE, CRB and FIM matrices under mismatched situation, and

$$\begin{aligned}\boldsymbol{J}_{mis}(\boldsymbol{\theta}|\boldsymbol{\alpha}) = {} & \mathbb{E}_{p_1(\boldsymbol{r}|\boldsymbol{\theta},\boldsymbol{\alpha})}\Big\{\Big(\frac{p_0(\boldsymbol{r}|\boldsymbol{\theta},\boldsymbol{\alpha})}{p_1(\boldsymbol{r}|\boldsymbol{\theta},\boldsymbol{\alpha})}\Big)^2 \\ & \times \nabla_{\boldsymbol{\theta}}\log p_0(\boldsymbol{r}|\boldsymbol{\theta},\boldsymbol{\alpha})[\nabla_{\boldsymbol{\theta}}\log p_0(\boldsymbol{r}|\boldsymbol{\theta},\boldsymbol{\alpha})]^{\dagger}\Big\} \end{aligned} \quad (59)$$

Next note that $\nabla_{\boldsymbol{\theta}}\log p(\boldsymbol{r}|\boldsymbol{\theta},\boldsymbol{\alpha}) = (\nabla_{\theta}\boldsymbol{\vartheta}^{\dagger})\nabla_{\boldsymbol{\vartheta}}\log p(\boldsymbol{r}|\boldsymbol{\vartheta},\boldsymbol{\alpha})$ and $p_0(\boldsymbol{r}|\boldsymbol{\theta},\boldsymbol{\alpha}) = p_0(\boldsymbol{r}|\boldsymbol{\vartheta},\boldsymbol{\alpha})$ so that

$$\boldsymbol{J}_{mis}(\boldsymbol{\theta}|\boldsymbol{\alpha}) = (\nabla_{\boldsymbol{\theta}}\boldsymbol{\vartheta}^{\dagger})\boldsymbol{J}_{mis}(\boldsymbol{\vartheta}|\boldsymbol{\alpha})(\nabla_{\boldsymbol{\theta}}\boldsymbol{\vartheta}^{\dagger})^{\dagger}, \quad (60)$$

where

$$\boldsymbol{J}_{mis}(\boldsymbol{\vartheta}|\boldsymbol{\alpha}) = \mathbb{E}_{p_1(\boldsymbol{r}|\boldsymbol{\vartheta},\boldsymbol{\alpha})}\left\{\left(\frac{p_0(\boldsymbol{r}|\boldsymbol{\vartheta},\boldsymbol{\alpha})}{p_1(\boldsymbol{r}|\boldsymbol{\vartheta},\boldsymbol{\alpha})}\right)^2 \times \nabla_{\boldsymbol{\vartheta}} \log p_0(\boldsymbol{r}|\boldsymbol{\vartheta},\boldsymbol{\alpha})[\nabla_{\boldsymbol{\vartheta}} \log p_0(\boldsymbol{r}|\boldsymbol{\vartheta},\boldsymbol{\alpha})]^{\dagger}\right\} \quad (61)$$

Calculation of the derivatives and further simplification of (61) is omitted due to similarity to the case without mismatch.

V. Numerical Examples

In this section, examples are presented which demonstrate the use of the GCRB and the mismatched CRB presented in the previous section to bound the performance of distributed radar networks which employ multiple widely spaced transmitters and receivers to jointly estimate target position and velocity. For brevity, we focus on examples which employ signals that are more applicable for passive radar. Initially, we describe performance when the transmitted signals are either known or where the transmitted signals of opportunity are estimated perfectly from a direct path reception. Later we consider cases where this is not true. We also assume that the positions of the transmitters and receivers are exactly known. For passive radar cases, these assumptions allow us to describe the best possible performance that can be obtained under the best circumstances.

It is easy to employ our bounds for cases where all parameters to be included in the vector $\boldsymbol{\alpha}$ are known and thus the bound in (55) is applicable. However, the vector $\boldsymbol{\alpha}$ might include a random bit sequence which contains information being transmitted. In order to avoid presenting a CRB for every possible bit sequence (α), we quote the expected CRB averaged over all bit sequences (ECRBOB), assuming each bit sequence to be perfectly estimated. From (55),

$$ECRBOB(\boldsymbol{\theta}) = \mathbb{E}_{\boldsymbol{\alpha}}\{CRB(\boldsymbol{\theta}|\boldsymbol{\alpha})\} \quad (62)$$

clearly bounds the corresponding covariance matrrix averaged over all bit sequences. For the best case, when the bit sequence in $\boldsymbol{\alpha}$ is perfectly estimated, the ECRBOB is a good indicator of performance. For example, it describes how the system parameters, such as the number of antennas, the geometry, and the waveforms impact performance, assuming accurate estimation of $\boldsymbol{\alpha}$. One can use the ECRBOB to optimize any parameter of interest.

Consider a target moving with velocity $(50, 30)$ m/s is present at $(15.15, 10.1275)$ km. To define a general test set up that is easy to describe for general M and N, each transmit and receive (single antenna) station is located 7 km from the reference point (15,10) km. The M transmit stations are uniformly distributed in angle over the range $[0, 2\pi)$, i.e, the angle of the m-th transmitter is $\varphi_m^t = 2\pi(m-1)/M, m = 1, \cdots, M$. The N receive stations are also uniformly distributed in angle over the range $[0, 2\pi)$, i.e. the angle of the n-th receive station is $\varphi_n^r = 2\pi(n-1)/N, n = 1, \cdots, N$, where the angles are measured with respect to the horizontal axis originated at the reference point as illustrated in Figure 1. Suppose $E_1 = E_2 = ... = E_M = E$. Fix $SCNR = 10\log((\sum_{n=1}^{N}\sum_{m=1}^{M}\sigma_{nm}^2 E P_0/d_{tm}^2 d_{rn}^2)/(N\sigma_w^2)$, called the signal-to-clutter-plus-noise ratio (SCNR), where $\sigma_{nm}^2 = \mathbb{E}\{\zeta_{nm}\zeta_{nm}^H\}$

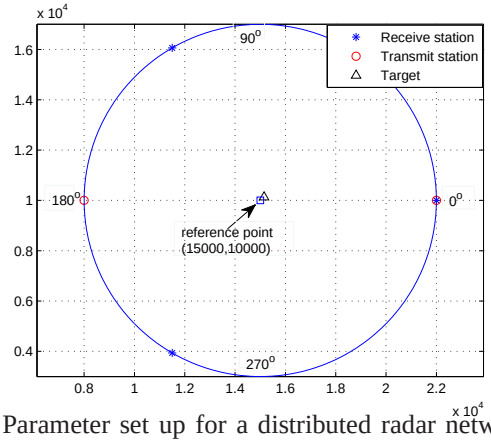

Fig. 1: Parameter set up for a distributed radar network with $M = 2$ and $N = 3$.

and $\sigma_w^2 = \mathbb{E}\{w_n(1)w_n(1)^H\} = \cdots = \mathbb{E}\{w_n(K)w_n(K)^H\}$. We set $\sigma_{nm}^2 = 1$ for all n and m, and $P_0 = 1$.

To be relevant to a passive radar system, the signals considered are those employed by the popular Global System for Mobile (GSM) Communications system. The baseband transmitted waveforms are Gaussian minimum shift keying (GMSK) signals [13]

$$s_m(k, \boldsymbol{\alpha}_m) = A_m \exp\left\{j\sum_{i=1}^{N_c} c_{mi}\sum_{j=1}^{k} z(kT_s - iT_p)T_s\right\} e^{j2\pi m\triangle f k T_s}, \quad (63)$$

where $\boldsymbol{\alpha}_m = \left[c_{m1}, \ldots, c_{mN_c}\right]^{\dagger}$,

$$z(t) = \frac{\pi}{2T_p}\left\{\vartheta\left[\frac{2\pi B}{\sqrt{\ln 2}}(t - T_P)\right] - \vartheta\left[\frac{2\pi B}{\sqrt{\ln 2}}t\right]\right\}, \quad (64)$$

$\vartheta[t] = \left(1/\sqrt{2\pi}\right)\int_t^{\infty} e^{-\tau^2/2}d\tau$, T_p is the bit duration, B denotes the 3 dB bandwidth of the Gaussian prefilter used in the GMSK modulators, $c_{mi} \in \{-1, 1\}$ is the ith ($i = 1, \ldots, N_c$) binary data bit of the mth transmitted waveform, N_c denotes the number of bits contained in the observation interval, A_m is the normalization factor, and $\triangle f = f_{k+1} - f_k$ is the frequency offset between different signals of opportunity with neighboring frequencies. In the simulations, we generate $c_{mi} = -1$ or 1 randomly with the same probability of 0.5. To model a GSM system, assume $T_p = 577\mu s, BT_p = 0.3, N_c = 16$, the carrier frequency $f_c = 900$ MHz and $\triangle f = 3$ KHz (orthogonal signals) or $\triangle f = 300$ Hz (nonorthogonal signals). It should be noticed that the bandwidth is only 520Hz and $N_c = 16$ in the simulation because of the huge calculation complexity.

Figure 2 shows the cases with $M = 2$, $N = 3$ and $M = 5$, $N = 4$ for spatially independent refection coefficients, spatially independent noise, and nonorthogonal signals. The solid and dashed curves show the root ECRBOB (RECRBOB) and the root mean squared error (RMSE) of the ML estimation, respectively, in the cases investigated. It is seen that all curves show that the RMSE decreases as the signal-to-clutter-plus-noise ratio (SCNR) is increased. In support of the correctness of our derived CRBs, all RMSE curves show the existence of a

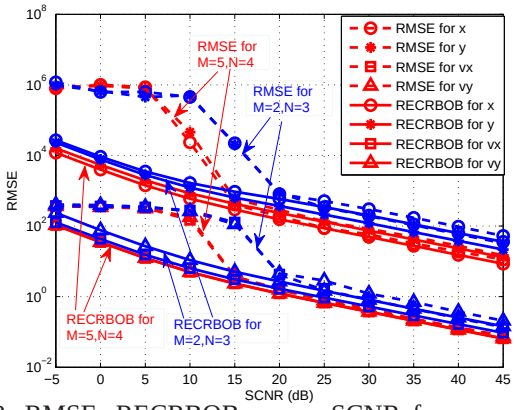

Fig. 2: RMSE, RECRBOB versus SCNR for a passive distributed radar network with $M = 2$, $N = 3$ and $M = 5$, $N = 4$, spatially independent refection coefficients, spatially independent noise, and nonorthogonal signal.

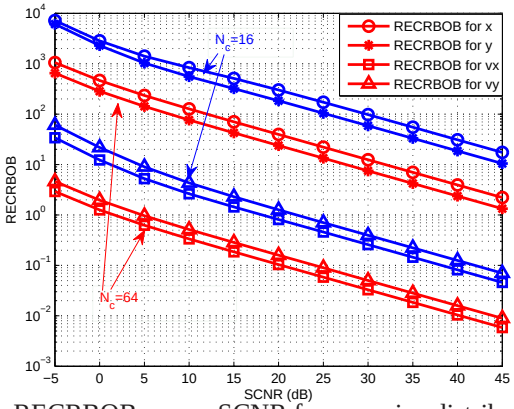

Fig. 3: RECRBOB versus SCNR for a passive distributed radar network with $M = 2$, $N = 3$, spatially independent refection coefficients, spatially independent noise, and orthogonal signals.

threshold, above which the RMSE starts to become close to the RECRBOB in value and slope. We can see that the threshold in the case with $M = 5$, $N = 4$ is 15 dB, while the threshold in the case with $M = 2$, $N = 3$ is 20 dB. The MSE curves for $M = 5$, $N = 4$ have a significantly lower threshold than those for $M = 2$, $N = 3$, apparently due to the additional transmit and receive stations, while the reduction in RECRBOB and the RMSE above threshold due to employing $M = 5$, $N = 4$ instead of $M = 2$, $N = 3$ is significantly smaller. Also, in the high SCNR region, RMSE is closer to RECRBOB for the case with $M = 5$, $N = 4$ than for the case with $M = 2$, $N = 3$.

Increasing the time duration of the signals, N_c in (63) also provides benefits as one would expect. While Figure 2 considers the case of $N_c = 16$, Figure 3 shows a comparison between RECRBOB for $N_c = 16$ and RECRBOB for $N_c = 64$ for the same case of $M = 2$, $N = 3$, spatially independent refection coefficients, spatially independent noise, and orthogonal signals. Here we can see that if we increase N_c, the RECRBOB will be significant reduced. In the following cases, to reduce complexity, we employ $N_c = 16$.

1) Orthogonal Signals and Nonorthogonal Signals: In this section, we focus on the effect of the nonorthogonality of the different transmitted signals. We consider the situation of spatially independent reflection coefficients, spatially independent noise, and nonorthogonal signals. The other factors are the same as in Figure 2. The system considered in Figure 4 has $M = 2$ transmitters and $N = 3$ receivers. The red and blue curves in this figure correspond to the cases with orthogonal and nonorthogonal signals, respectively. We see that the threshold obtained using the orthogonal signals is 15 dB while the threshold obtained using the nonorthogonal signals is 20 dB. Thus the threshold for the nonorthogonal signals tested is higher than the threshold for the orthogonal signals tested. It is also seen that the RECRBOB of the orthogonal signals tested is smaller than that for the nonorthogonal signals tested over the whole region of SCNR shown. So both the RMSE and RECRBOB indicate that the radar can achieve better

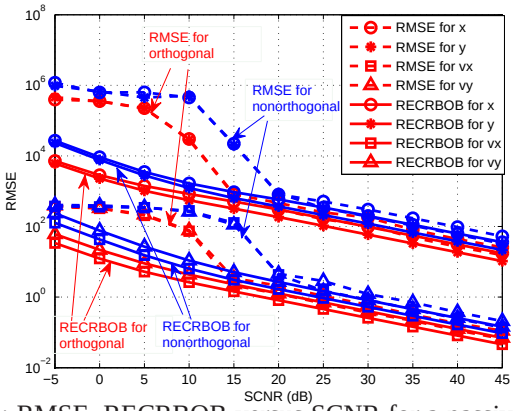

Fig. 4: RMSE, RECRBOB versus SCNR for a passive MIMO radar with $M = 2$ and $N = 3$, spatially independent refection coefficients, and spatially independent noise.

performance if the waveforms are closer to being orthogonal in the case considered.

2) Spatially Dependent Reflection Coefficients: In this section, we consider the situation of spatially dependent reflection coefficients, spatially independent noise, and orthogonal signals. The elements of the covariance matrix $\boldsymbol{R}$ describing the correlation between the different reflection coefficients are generated with [24]

$$\boldsymbol{R} = \boldsymbol{R}^r \otimes \boldsymbol{R}^t \tag{65}$$

where

$$\boldsymbol{R}^r = \begin{bmatrix} \rho^r_{11} & \cdots & \rho^r_{1N} \\ \vdots & \ddots & \vdots \\ \rho^r_{N1} & \cdots & \rho^r_{NN} \end{bmatrix}, \tag{66}$$

$$\rho^r_{nn'} = \exp\left(-\varpi \Delta\phi^r_{nn'}\right), \tag{67}$$

$$\boldsymbol{R}^t = \begin{bmatrix} \rho^t_{11} & \cdots & \rho^t_{1M} \\ \vdots & \ddots & \vdots \\ \rho^t_{M1} & \cdots & \rho^t_{MM} \end{bmatrix}, \tag{68}$$

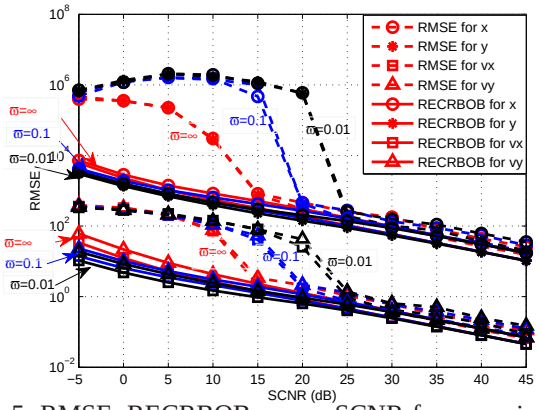

Fig. 5: RMSE, RECRBOB versus SCNR for a passive MIMO radar with $M = 2$ and $N = 3$, spatially dependent reflection coefficients, spatially independent noise, and orthogonal signals.

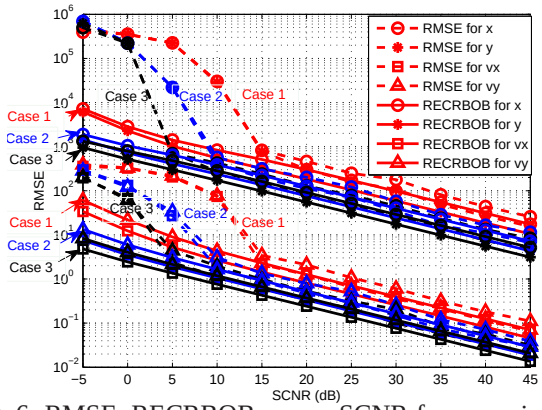

Fig. 6: RMSE, RECRBOB versus SCNR for a passive MIMO radar with $M = 2$ and $N = 3$, spatially independent reflection coefficients, dependent noise, and orthogonal signals.

and

$$\rho^t_{mm'} = \exp\left(-\varpi \Delta\phi^t_{mm'}\right). \tag{69}$$

The symbol $\Delta\phi^r_{nn'}$ denotes the separation angle between the nth and n'th transmitter-to-target paths, $\Delta\phi^t_{mm'}$ denotes the separation angle between the mth and m'th target-to-receiver paths, and ϖ sets the exponential decay in correlation with angle. From the model, it is easy to see that larger ϖ implies less dependency for fixed $\Delta\phi^r_{nn'}$ and $\Delta\phi^t_{mm'}$. We consider $\varpi = 0.01$, 0.1, and ∞ in the figures. Here $\varpi = \infty$ implies that the reflection coefficients are independent.

Figure 5 shows the comparison of RECRBOB and RMSE for different ϖ when all of the other parameters are the same as in Figure 2. We can see that the thresholds for the cases with $\varpi = \infty$, 0.1, and 0.01 are 15 dB, 20 dB and 25 dB, respectively. Thus, less dependency leads to a more favorable threshold such that the RECRBOB is achievable at lower SCNR. Above threshold, all the curves are relatively close. The results imply that the dependency of the reflection coefficients does not have tremendous impact on the radar estimation performance, provided we operate above threshold. However, with less dependency the radar can operate at lower SCNR while still achieving an acceptable performance level.

3) Gaussian Spatially Dependent Noise: In this section, we consider the situation of spatially independent reflection coefficients, spatially dependent noise, and orthogonal signals. The elements of the noise covariance matrix $\boldsymbol{Q}$ are generated with the following model

$$\boldsymbol{Q} = \sigma_w^2 \tilde{\boldsymbol{Q}} \otimes \boldsymbol{I}_K, \tag{70}$$

where the nn'th element of $\tilde{\boldsymbol{Q}}$ is assumed to be

$$\tilde{Q}_{nn'} = \exp\{-d_{nn'}\gamma\} \tag{71}$$

where $d_{nn'} = \sqrt{\left(x^r_n - x^r_{n'}\right)^2 + \left(y^r_n - y^r_{n'}\right)^2}$, γ sets the exponential decay in correlation with distance, and $\boldsymbol{I}_K$ denotes a $K \times K$ identity matrix. From the model we can see larger γ results in less dependency for fixed $d_{nn'}$. We consider the situations of $\gamma = 0.000005$, 0.00001, and ∞ and assume all the other parameters are the same as in Figure 2. Here $\gamma = \infty$ implies that the noise components are independent.

Figure 6 shows the comparison of the RECRBOB and RMSE for different values of γ. Case 1, Case 2 and Case 3 respectively represents $\gamma = \infty$, 0.00001, and 0.000005. It is observed that the thresholds for cases with $\gamma = \infty$, 0.00001, and 0.000005 are 15 dB, 10 dB, and 5 dB, respectively. Thus, more dependency leads to a more favorable threshold such that the RECRBOB is achievable at lower SCNR. Above the threshold, we see that $\gamma = 0.000005$ has the smallest RECRBOB while $\gamma = \infty$ has the largest RECRBOB, which means larger dependency can lead to lower RECRBOB. In the cases considered in Figure 6, correlated noise leads to better performance.

4) Inaccurate Signal Estimation: Now consider the case where the transmitted signals are not estimated perfectly, possibly from the direct path receptions. Let $n_{nm}(k), n = 1, \cdots, N, m = 1, \cdots, M, k = 1, \cdots, K$ denote an independent and identically distributed sequence of complex Gaussian noise samples, each with zero mean and variance 0.1 which models the estimation error in the signal using

$$u_{nm}(k) = \sqrt{\frac{E_m P_0}{d^2_{tm} d^2_{rn}}}[s_m(kT_s - \tau_{nm}, \boldsymbol{\alpha}_m) + n_{nm}(k)]e^{j2\pi f_{nm} k T_s} \tag{72}$$

Then (72) is used to form $\boldsymbol{S}$ with the equations (9), (10), (13) already given in the paper, and we call this mismatched $\boldsymbol{S}$ $\boldsymbol{S_0}$. The undistorted $\boldsymbol{S}$ obtained this way, but without additive noise, is called $\boldsymbol{S_1}$. This is exactly a case where the model we employ in our estimation algorithm is mismatched so the $\text{RECRBOB}_{\text{mis}}$ results from Section IV become applicable. The resulting average $\text{RECRBOB}_{\text{mis}}$ and RMSE_{mis}, after averaging over the noise using a Monte Carlo simulation, are plotted in Figure 7. From the figure, we can see that the $\text{RECRBOB}_{\text{mis}}$ provides an informative lower bound[1] on RMSE_{mis} in this case.

[1]We have verified that the unaveraged values of $\text{RECRBOB}_{\text{mis}}$ also provide a lower bound to the unaveraged values of RMSE_{mis}.

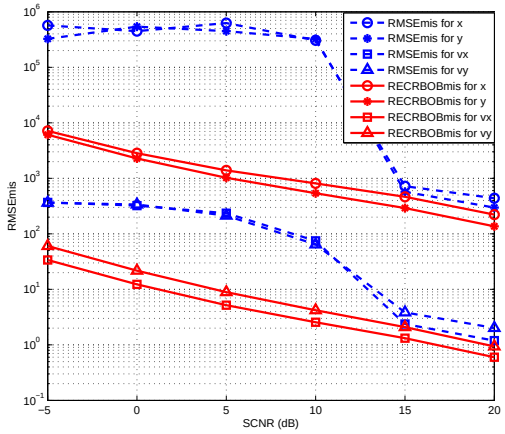

Fig. 7: RMSEmis, RECRBOBmis versus SCNR for a passive MIMO radar with $M = 2$ and $N = 3$, spatially independent reflection coefficients, independent noise, and orthogonal signals.

Note that all the other details of the system analyzed in Figure 7, except for this signal mismatch, are the same as in Figure 2.

VI. Conclusions

In this paper, we studied the performance of joint target position and velocity estimation using a distributed radar network under more general conditions than assumed in previous work. A received signal model has been developed for active and passive radar with M transmit and N receive stations. The ML estimate and the exact CRB expression are derived for possibly nonorthogonal signals, spatially dependent Gaussian reflection coefficients, and spatially dependent Gaussian clutter-plus-noise. For cases in which some parameters (for example the transmitted signal from direct path reception) are not estimated correctly, we also derive the mismatched CRB. Numerical results are given to illustrate the use of the CRB and mismatched CRB. The numerical results show various cases with signals of opportunity taken from a GSM wireless communication system. It was shown that in the particular cases investigated, the nonorthogonality of signal degraded the estimation performance both in terms of RECRBOB and in terms of the threshold above which the RMSE starts to become close to the RECRBOB in value and slope. Decreasing the dependency between the different reflection coefficients led to a more favorable threshold such that the radar can operate at lower SCNR while still achieving an acceptable performance level. Above threshold the dependency of the reflection coefficients had little impact on the estimation performance, provided a well performing estimation approach (nearly CRB achieving) is employed. In some specific examples, it was also shown that an increase in the dependency between the noise samples at different antennas led to better estimation performance in terms of the threshold and RECRBOB.

The work here can be generalized in several directions. The CRB, a tight bound only for the high SCNR region and being limited to unbiased estimators, is incapable of characterizing the threshold value or accurately describing the low-SCNR estimation performance of estimators. In this regard, we need better analytical tools which can predict estimation performance for low SCNR. The Ziv-Zakai bound is one promising approach, which will be studied in our future work. The Ziv-Zakai bound also allows prior information to be incorporated into the estimation.

Appendix A
Calculation of $\boldsymbol{J}(\boldsymbol{\vartheta}|\boldsymbol{\alpha})$

According to (23) and (43), we can obtain the FIM of the vector $\boldsymbol{\vartheta}$ as

$$\boldsymbol{J}(\boldsymbol{\vartheta}|\boldsymbol{\alpha}) = \begin{bmatrix} \boldsymbol{J}_{\tau\tau} & \boldsymbol{J}_{\tau f} & \boldsymbol{J}_{\tau d_t} & \boldsymbol{J}_{\tau d_r} \\ \boldsymbol{J}_{f\tau} & \boldsymbol{J}_{ff} & \boldsymbol{J}_{f d_t} & \boldsymbol{J}_{f d_r} \\ \boldsymbol{J}_{d_t\tau} & \boldsymbol{J}_{d_t f} & \boldsymbol{J}_{d_t d_t} & \boldsymbol{J}_{d_t d_r} \\ \boldsymbol{J}_{d_r\tau} & \boldsymbol{J}_{d_r f} & \boldsymbol{J}_{d_r d_t} & \boldsymbol{J}_{d_r d_r} \end{bmatrix}, \tag{73}$$

where $\boldsymbol{J}_{\tau\tau} = \boldsymbol{J}_{\tau}^H \boldsymbol{J}_{\tau}$, $\boldsymbol{J}_{\tau f} = \boldsymbol{J}_{f\tau}^H = \boldsymbol{J}_{\tau}^H \boldsymbol{J}_f$, $\boldsymbol{J}_{\tau d_t} = \boldsymbol{J}_{d_t\tau}^H = \boldsymbol{J}_{\tau}^H \boldsymbol{J}_{d_t}$, $\boldsymbol{J}_{\tau d_r} = \boldsymbol{J}_{d_r\tau}^H = \boldsymbol{J}_{\tau}^H \boldsymbol{J}_{d_r}$, $\boldsymbol{J}_{ff} = \boldsymbol{J}_f^H \boldsymbol{J}_f$, $\boldsymbol{J}_{f d_t} = \boldsymbol{J}_{d_t f}^H = \boldsymbol{J}_f^H \boldsymbol{J}_{d_t}$, $\boldsymbol{J}_{f d_r} = \boldsymbol{J}_{d_r f}^H = \boldsymbol{J}_f^H \boldsymbol{J}_{d_r}$, $\boldsymbol{J}_{d_t d_t} = \boldsymbol{J}_{d_t}^H \boldsymbol{J}_{d_t}$, $\boldsymbol{J}_{d_t d_r} = \boldsymbol{J}_{d_r d_t}^H = \boldsymbol{J}_{d_t}^H \boldsymbol{J}_{d_r}$, $\boldsymbol{J}_{d_r d_r} = \boldsymbol{J}_{d_r}^H \boldsymbol{J}_{d_r}$,

$$\boldsymbol{J}_{\boldsymbol{\tau}} = \left(\boldsymbol{C}^{-\dagger/2} \otimes \boldsymbol{C}^{-1/2}\right) \frac{\partial \boldsymbol{C}_{vec}}{\partial \boldsymbol{\tau}^{\dagger}}, \tag{74}$$

$$\boldsymbol{J}_{\boldsymbol{f}} = \left(\boldsymbol{C}^{-\dagger/2} \otimes \boldsymbol{C}^{-1/2}\right) \frac{\partial \boldsymbol{C}_{vec}}{\partial \boldsymbol{f}^{\dagger}}, \tag{75}$$

$$\boldsymbol{J}_{\boldsymbol{d_t}} = \left(\boldsymbol{C}^{-\dagger/2} \otimes \boldsymbol{C}^{-1/2}\right) \frac{\partial \boldsymbol{C}_{vec}}{\partial \boldsymbol{d_t}^{\dagger}}, \tag{76}$$

and

$$\boldsymbol{J}_{\boldsymbol{d_r}} = \left(\boldsymbol{C}^{-\dagger/2} \otimes \boldsymbol{C}^{-1/2}\right) \frac{\partial \boldsymbol{C}_{vec}}{\partial \boldsymbol{d_r}^{\dagger}}. \tag{77}$$

Then we reformulate the $\boldsymbol{J}(\boldsymbol{\vartheta}|\boldsymbol{\alpha})$ in a somewhat more explicit matrix form.

First we derive $\boldsymbol{J}_{\boldsymbol{\tau\tau}}$, let $\boldsymbol{s}_i$ and $\boldsymbol{z}_i$ denote the ith column of $\boldsymbol{S}$ and $\boldsymbol{R}$, respectively, such that $\boldsymbol{S} = [\boldsymbol{s}_1, \cdots, \boldsymbol{s}_{MN}]$ and $\boldsymbol{R} = [\boldsymbol{z}_1, \cdots, \boldsymbol{z}_{MN}]$. Note that $\boldsymbol{R}$ is a Hermitian matrix, i.e., $\boldsymbol{R} = [\boldsymbol{z}_1, \cdots, \boldsymbol{z}_{MN}]^H$. Then, we have

$$\begin{aligned} \frac{\partial \boldsymbol{C}}{\partial \tau_{nm}} &= \frac{\partial \left(\boldsymbol{S}\boldsymbol{R}\boldsymbol{S}^H + \boldsymbol{Q}\right)}{\partial \tau_{nm}} \\ &= \frac{\partial \boldsymbol{S}}{\partial \tau_{nm}} \boldsymbol{R}\boldsymbol{S}^H + \boldsymbol{S}\boldsymbol{R} \frac{\partial \boldsymbol{S}^H}{\partial \tau_{nm}} \\ &= \boldsymbol{s}_i^{\tau} \boldsymbol{z}_i^H \boldsymbol{S}^H + \boldsymbol{S}\boldsymbol{z}_i (\boldsymbol{s}_i^{\tau})^H, \end{aligned} \tag{78}$$

where $i = M(n-1) + m$ for $n = 1, \cdots, N$ and $m = 1, \cdots, M$,

$$\boldsymbol{s}_i^{\tau} = \frac{\partial \boldsymbol{s}_i}{\partial \tau_{nm}} = \boldsymbol{e}_n \otimes \left[\frac{\partial u_{nm}(1)}{\partial \tau_{nm}}, \cdots, \frac{\partial u_{nm}(K)}{\partial \tau_{nm}}\right]^{\dagger}, \tag{79}$$

where $\boldsymbol{e}_n$ is an $N \times 1$ column vector with zero everywhere except for a 1 in the nth entry and

$$\frac{\partial u_{nm}(k)}{\partial \tau_{nm}} = \sqrt{\frac{E_m P_0}{d_{tm}^2 d_{rn}^2}} \frac{\partial s_m(kT_s - \tau_{nm}, \boldsymbol{\alpha}_m)}{\partial \tau_{nm}} e^{j2\pi f_{nm} k T_s}. \tag{80}$$

According to the following identity [30]

$$\left(\boldsymbol{X}^{\dagger}\otimes\boldsymbol{A}\right)\mathrm{vec}\left(\boldsymbol{B}\right)=\mathrm{vec}\left(\boldsymbol{ABX}\right), \tag{81}$$

we can obtain

$$\begin{aligned}\boldsymbol{J}_{\tau_{nm}}=&\left(\boldsymbol{C}^{-\dagger/2}\otimes\boldsymbol{C}^{-1/2}\right)\frac{\partial\mathrm{vec}\left(\boldsymbol{C}\right)}{\partial\tau_{nm}}\\ =&\mathrm{vec}\left(\boldsymbol{C}^{-1/2}\frac{\partial\boldsymbol{C}}{\partial\tau_{nm}}\boldsymbol{C}^{-1/2}\right)\\ =&\ \mathrm{vec}\left\{\boldsymbol{C}^{-1/2}\left(\boldsymbol{s}_i^{\tau}\boldsymbol{z}_i^{H}\boldsymbol{S}^{H}+\boldsymbol{S}\boldsymbol{z}_i(\boldsymbol{s}_i^{\tau})^{H}\right)\boldsymbol{C}^{-1/2}\right\}\\ =&\mathrm{vec}\left(\boldsymbol{V}_i+\boldsymbol{V}_i^{H}\right),\end{aligned} \tag{82}$$

where $\boldsymbol{V}_i=\boldsymbol{C}^{-1/2}\boldsymbol{s}_i^{\tau}\boldsymbol{z}_i^{H}\boldsymbol{S}^{H}\boldsymbol{C}^{-1/2}$. Using (82) and the following identity [30]

$$\mathrm{vec}\left(\boldsymbol{A}^{\dagger}\right)^{\dagger}\mathrm{vec}\left(\boldsymbol{B}\right)=Tr\left(\boldsymbol{AB}\right)=Tr\left(\boldsymbol{BA}\right), \tag{83}$$

we can derive the ijth element of $\boldsymbol{J}^{\boldsymbol{\tau\tau}}$ as follows

$$\begin{aligned}&[\boldsymbol{J}_{\boldsymbol{\tau\tau}}]_{ij}=\mathrm{vec}\left\{\boldsymbol{V}_i+\boldsymbol{V}_i^{H}\right\}^{H}\mathrm{vec}\left\{\boldsymbol{V}_j+\boldsymbol{V}_j^{H}\right\}\\ &=\mathrm{Tr}\left\{\left(\boldsymbol{V}_i+\boldsymbol{V}_i^{H}\right)\left(\boldsymbol{V}_j+\boldsymbol{V}_j^{H}\right)\right\}\\ &=2\Re\{Tr(V_iV_j+V_i^{H}V_j)\}\\ &=2\Re\left\{\boldsymbol{z}_i^{H}\boldsymbol{S}^{H}\boldsymbol{C}^{-1}\boldsymbol{s}_j^{\tau}\boldsymbol{z}_j^{H}\boldsymbol{S}^{H}\boldsymbol{C}^{-1}\boldsymbol{s}_i^{\tau}+(\boldsymbol{s}_i^{\tau})^{H}\boldsymbol{C}^{-1}\boldsymbol{s}_j^{\tau}\boldsymbol{z}_j^{H}\boldsymbol{S}^{H}\boldsymbol{C}^{-1}\boldsymbol{S}\boldsymbol{z}_i\right\},\end{aligned} \tag{84}$$

where $j=M(n'-1)+m'$ for $n'=1,\cdots,N$ and $m'=1,\cdots,M$. Then, according to (84), we can reformulate $\boldsymbol{J}_{\boldsymbol{\tau\tau}}$ in the form of a matrix

$$\boldsymbol{J}_{\boldsymbol{\tau\tau}}=2\Re\left\{\boldsymbol{YS}^{\boldsymbol{\tau}}\odot(\boldsymbol{YS}^{\boldsymbol{\tau}})^{\dagger}+(\boldsymbol{S}^{\boldsymbol{\tau}})^{H}\boldsymbol{C}^{-1}\boldsymbol{S}^{\boldsymbol{\tau}}\odot(\boldsymbol{YSR})^{\dagger}\right\}, \tag{85}$$

where $\boldsymbol{S}^{\boldsymbol{\tau}}=\left[\boldsymbol{s}_1^{\tau},\cdots,\boldsymbol{s}_{MN}^{\tau}\right]$ and $\boldsymbol{Y}=\boldsymbol{RS}^{H}\boldsymbol{C}^{-1}$. Similarly, we can obtain

$$\boldsymbol{J}_{\boldsymbol{\tau f}}=2\Re\left\{\boldsymbol{YS}^{\boldsymbol{f}}\odot(\boldsymbol{YS}^{\boldsymbol{\tau}})^{\dagger}+(\boldsymbol{S}^{\boldsymbol{\tau}})^{H}\boldsymbol{C}^{-1}\boldsymbol{S}^{\boldsymbol{f}}\odot(\boldsymbol{YSR})^{\dagger}\right\}, \tag{86}$$

and

$$\boldsymbol{J}_{\boldsymbol{ff}}=2\Re\left\{\boldsymbol{YS}^{\boldsymbol{f}}\odot\left(\boldsymbol{YS}^{\boldsymbol{f}}\right)^{\dagger}+\left(\boldsymbol{S}^{\boldsymbol{f}}\right)^{H}\boldsymbol{C}^{-1}\boldsymbol{S}^{\boldsymbol{f}}\odot(\boldsymbol{YSR})^{\dagger}\right\}, \tag{87}$$

where $\boldsymbol{S}^{\boldsymbol{f}}=\left[\boldsymbol{s}_1^{\boldsymbol{f}},\cdots,\boldsymbol{s}_{MN}^{\boldsymbol{f}}\right]$,

$$\boldsymbol{s}_i^{\boldsymbol{f}}=\frac{\partial\boldsymbol{s}_i}{\partial f_{nm}}=\boldsymbol{e}_n\otimes\left[\frac{\partial u_{nm}(1)}{\partial f_{nm}},\cdots,\frac{\partial u_{nm}(K)}{\partial f_{nm}}\right]^{\dagger}, \tag{88}$$

and

$$\frac{\partial u_{nm}(k)}{\partial f_{nm}}=j2\pi kT_s u_{nm}(k). \tag{89}$$

Next we derive $\boldsymbol{J}_{\boldsymbol{d}_t}$,

$$\begin{aligned}&\frac{\partial\boldsymbol{C}}{\partial d_{tm}}=\frac{\partial(\boldsymbol{SRS}^{H}+\boldsymbol{Q})}{\partial d_{tm}}\\ &=\frac{\partial\boldsymbol{S}}{\partial d_{tm}}\boldsymbol{RS}^{H}+\boldsymbol{SR}\frac{\partial\boldsymbol{S}^{H}}{\partial d_{tm}}\\ &=(\boldsymbol{s}_m^{t}\boldsymbol{z}_m^{H}+\boldsymbol{s}_{m+M}^{t}\boldsymbol{z}_{m+M}^{H}+\cdots+\boldsymbol{s}_{m+(N-1)M}^{t}\boldsymbol{z}_{m+(N-1)M}^{H})\boldsymbol{S}^{H}\\ &+\boldsymbol{S}(\boldsymbol{z}_m(\boldsymbol{s}_m^{t})^{H}+\boldsymbol{z}_{m+M}(\boldsymbol{s}_{m+M}^{t})^{H}+\cdots+\boldsymbol{z}_{m+(N-1)M}(\boldsymbol{s}_{m+(N-1)M}^{t})^{H}),\end{aligned} \tag{90}$$

where

$$\begin{aligned}&\boldsymbol{s}_{m+(n-1)M}^{t}=\frac{\partial\boldsymbol{s}_{m+(n-1)M}}{\partial d_{tm}}\\ &=\boldsymbol{e}_n\otimes[\frac{\partial u_{nm}(1)}{\partial d_{tm}},\frac{\partial u_{nm}(2)}{\partial d_{tm}}\cdots,\frac{\partial u_{nm}(K)}{\partial d_{tm}}]^{\dagger},\ n=1,\cdots,N\end{aligned} \tag{91}$$

and

$$\frac{\partial u_{nm}(k)}{\partial d_{tm}}=-\frac{\sqrt{E_mP_0}}{d_{tm}^{2}d_{rn}}s(kT_s-\tau_{nm},\boldsymbol{\alpha}_m)e^{j2\pi f_{nm}kT_s}. \tag{92}$$

It can be derived that

$$\begin{aligned}\boldsymbol{J}_{d_{tm}}=&(\boldsymbol{C}^{-\dagger/2}\otimes\boldsymbol{C}^{-1/2})\frac{\partial\boldsymbol{C}_{vec}}{\partial d_{tm}}\\ =&vec(\boldsymbol{C}^{-1/2}\frac{\partial\boldsymbol{C}}{\partial d_{tm}}\boldsymbol{C}^{-1/2})\\ =&vec\{\boldsymbol{C}^{-1/2}((\boldsymbol{s}_m^{t}\boldsymbol{z}_m^{H}+\boldsymbol{s}_{m+M}^{t}\boldsymbol{z}_{m+M}^{H}+\cdots\\ &+\boldsymbol{s}_{m+(N-1)M}^{t}\boldsymbol{z}_{m+(N-1)M}^{H})\boldsymbol{S}^{H}\\ &+\boldsymbol{S}(\boldsymbol{z}_m(\boldsymbol{s}_m^{t})^{H}+\boldsymbol{z}_{m+M}(\boldsymbol{s}_{m+M}^{t})^{H}+\cdots\\ &+\boldsymbol{z}_{m+(N-1)M}(\boldsymbol{s}_{m+(N-1)M}^{t})^{H}))\boldsymbol{C}^{-1/2}\}\\ =&vec(\ell_m+\ell_m^{H}),\end{aligned} \tag{93}$$

where $\ell_m=\boldsymbol{C}^{-1/2}(\boldsymbol{s}_m^{t}\boldsymbol{z}_m^{H}+\boldsymbol{s}_{m+M}^{t}\boldsymbol{z}_{m+M}^{H}+\cdots+\boldsymbol{s}_{m+(N-1)M}^{t}\boldsymbol{z}_{m+(N-1)M}^{H})\boldsymbol{S}^{H}\boldsymbol{C}^{-1/2}$. Then, we obtain

$$\begin{aligned}&[\boldsymbol{J}_{\boldsymbol{d}_t\boldsymbol{d}_t}]_{mm'}=vec(\ell_m+\ell_m^{H})^{H}vec(\ell_{m'}+\ell_{m'}^{H})\\ &=Tr\{(\ell_m+\ell_m^{H})(\ell_{m'}+\ell_{m'}^{H})\}\\ &=2\Re\{Tr(\ell_m\ell_{m'}+\ell_m^{H}\ell_{m'})\}\\ &=2\Re\{\sum_{n=1}^{N}\sum_{n'=1}^{N}((\boldsymbol{z}_{m+(n-1)M})^{H}\boldsymbol{S}^{H}\boldsymbol{C}^{-1}\boldsymbol{s}_{m'+(n'-1)M}^{t}(\boldsymbol{z}_{m'+(n'-1)M})^{H}\boldsymbol{S}^{H}\\ &\boldsymbol{C}^{-1}\boldsymbol{s}_{m+(n-1)M}^{t}+(\boldsymbol{s}_{m+(n-1)M}^{t})^{H}\boldsymbol{C}^{-1}\boldsymbol{s}_{m'+(n'-1)M}^{t}(\boldsymbol{z}_{m'+(n'-1)M})^{H}\boldsymbol{S}^{H}\\ &\boldsymbol{C}^{-1}\boldsymbol{S}\boldsymbol{z}_{m+(n-1)M})\}.\end{aligned} \tag{94}$$

Reformulate $\boldsymbol{J}_{\boldsymbol{d}_t\boldsymbol{d}_t}$ in the form of a matrix

$$\begin{aligned}\boldsymbol{J}_{\boldsymbol{d}_t\boldsymbol{d}_t}=&2\Re\{\sum_{n=1}^{N}\sum_{n'=1}^{N}(\boldsymbol{\aleph}_n\boldsymbol{S}^{H}\boldsymbol{C}^{-1}\Im_{n'}\odot(\boldsymbol{\aleph}_{n'}\boldsymbol{S}^{H}\boldsymbol{C}^{-1}\Im_n)^{\dagger}\\ &+(\Im_n)^{H}\boldsymbol{C}^{-1}\Im_{n'}\odot(\boldsymbol{\aleph}_{n'}\boldsymbol{S}^{H}\boldsymbol{C}^{-1}\boldsymbol{S}(\boldsymbol{\aleph}_n)^{H})^{\dagger})\},\end{aligned} \tag{95}$$

where $\boldsymbol{\aleph}_n=(\boldsymbol{z}_{1+(n-1)M},\cdots,\boldsymbol{z}_{M+(n-1)M})^{H}$, $\Im_n=(\boldsymbol{s}_{1+(n-1)M}^{t},\cdots,\boldsymbol{s}_{M+(n-1)M}^{t})$. Similarly, we can derive

$$\begin{aligned}\boldsymbol{J}_{\boldsymbol{d}_t\boldsymbol{\tau}}=&2\Re\{\sum_{n=1}^{N}(\boldsymbol{\aleph}_n\boldsymbol{S}^{H}\boldsymbol{C}^{-1}\boldsymbol{S}^{\boldsymbol{\tau}}\odot(\boldsymbol{RS}^{H}\boldsymbol{C}^{-1}\Im_n)^{\dagger}\\ &+(\Im_n)^{H}\boldsymbol{C}^{-1}\boldsymbol{S}^{\boldsymbol{\tau}}\odot(\boldsymbol{RS}^{H}\boldsymbol{C}^{-1}\boldsymbol{S}(\boldsymbol{\aleph}_n)^{H})^{\dagger})\},\end{aligned} \tag{96}$$

$$\begin{aligned}\boldsymbol{J}_{\boldsymbol{d}_t\boldsymbol{f}}=&2\Re\{\sum_{n=1}^{N}(\boldsymbol{\aleph}_n\boldsymbol{S}^{H}\boldsymbol{C}^{-1}\boldsymbol{S}^{\boldsymbol{f}}\odot(\boldsymbol{RS}^{H}\boldsymbol{C}^{-1}\Im_n)^{\dagger}\\ &+(\Im_n)^{H}\boldsymbol{C}^{-1}\boldsymbol{S}^{\boldsymbol{f}}\odot(\boldsymbol{RS}^{H}\boldsymbol{C}^{-1}\boldsymbol{S}(\boldsymbol{\aleph}_n)^{H})^{\dagger})\}.\end{aligned} \tag{97}$$

To derive d_{rn}, we employ

$$\begin{aligned}\frac{\partial C}{\partial d_{rn}} &= \frac{\partial(\boldsymbol{S}\boldsymbol{R}\boldsymbol{S}^H + \boldsymbol{Q})}{\partial d_{rn}} \\ &= \frac{\partial \boldsymbol{S}}{\partial d_{rn}}\boldsymbol{R}\boldsymbol{S}^H + \boldsymbol{S}\boldsymbol{R}\frac{\partial \boldsymbol{S}^H}{\partial d_{rn}} \\ &= (\boldsymbol{s}^r_{1+(n-1)M}\boldsymbol{z}^H_{1+(n-1)M} + \boldsymbol{s}^r_{2+(n-1)M}\boldsymbol{z}^H_{1+(n-1)M} + \cdots \\ &+ \boldsymbol{s}^r_{M+(n-1)M}\boldsymbol{z}^H_{M+(n-1)M})\boldsymbol{S}^H \\ &+ \boldsymbol{S}(\boldsymbol{z}_{1+(n-1)M}(\boldsymbol{s}^r_{1+(n-1)M})^H + \boldsymbol{z}_{2+(n-1)M}(\boldsymbol{s}^t_{2+(n-1)M})^H + \cdots + \boldsymbol{z}_{M+(n-1)M} \\ &(\boldsymbol{s}^t_{M+(n-1)M})^H), \end{aligned} \tag{98}$$

where

$$\begin{aligned}\boldsymbol{s}^r_{m+(n-1)M} &= \frac{\partial \boldsymbol{s}_{m+(n-1)M}}{\partial d_{rn}} \\ &= \boldsymbol{e}_n \otimes [\frac{\partial u_{nm}(1)}{\partial d_{rn}}, \frac{\partial u_{nm}(2)}{\partial d_{rn}} \cdots, \frac{\partial u_{nm}(K)}{\partial d_{rn}}]^\dagger,\ m = 1, \cdots, M, \end{aligned} \tag{99}$$

and

$$\frac{\partial u_{nm}(k)}{\partial d_{rn}} = -\frac{\sqrt{E_m P_0}}{d_{tm} d^2_{rn}} s(kT_s - \tau_{nm}, \boldsymbol{\alpha}_m) e^{j2\pi f_{nm} k T_s}, \tag{100}$$

We can then derive

$$\begin{aligned}\boldsymbol{J}_{d_{rn}} &= (\boldsymbol{C}^{-\dagger/2} \otimes \boldsymbol{C}^{-1/2})\frac{\partial \boldsymbol{C}_{vec}}{\partial d_{rn}} \\ &= vec(\boldsymbol{C}^{-1/2}\frac{\partial \boldsymbol{C}}{\partial d_{rn}}\boldsymbol{C}^{-1/2}) \\ &= vec\{\boldsymbol{C}^{-1/2}((\boldsymbol{s}^r_{1+(n-1)M}\boldsymbol{z}^H_{1+(n-1)M} + \boldsymbol{s}^r_{2+(n-1)M}\boldsymbol{z}^H_{2+(n-1)M} + \cdots \\ &+ \boldsymbol{s}^r_{M+(n-1)M}\boldsymbol{z}^H_{M+(n-1)M})\boldsymbol{S}^H \\ &+ \boldsymbol{S}((\boldsymbol{s}^r_{1+(n-1)M})^H\boldsymbol{z}_{1+(n-1)M} + (\boldsymbol{s}^t_{2+(n-1)M})^H\boldsymbol{z}_{2+(n-1)M} + \cdots \\ &+ (\boldsymbol{s}^t_{M+(n-1)M})^H\boldsymbol{z}_{M+(n-1)M}))\boldsymbol{C}^{-1/2}\} \\ &= vec(w_n + w^H_n), \end{aligned} \tag{101}$$

where $w_n = \boldsymbol{C}^{-1/2}(\boldsymbol{s}^r_{1+(n-1)M}\boldsymbol{z}^H_{1+(n-1)M} + \boldsymbol{s}^r_{2+(n-1)M}\boldsymbol{z}^H_{2+(n-1)M} + \cdots + \boldsymbol{s}^r_{M+(n-1)M}\boldsymbol{z}^H_{M+(n-1)M})\boldsymbol{S}^H\boldsymbol{C}^{-1/2}$.

Then, we can obtain

$$\begin{aligned}[\boldsymbol{J}_{\boldsymbol{d}_r\boldsymbol{d}_r}]_{nn'} &= vec(w_n + w^H_n)^H vec(w_{n'} + \ell^H_{n'}) \\ &= Tr\{(w_n + w^H_n)(w_{n'} + w^H_{n'})\} \\ &= 2\Re\{Tr(w_n w_{n'} + w^H_n w_{n'})\} \\ &= 2\Re\{\sum_{m=1}^{M}\sum_{m'=1}^{M}((\boldsymbol{z}_{m+(n-1)M})^H\boldsymbol{S}^H\boldsymbol{C}^{-1}\boldsymbol{s}^t_{m'+(n'-1)M}(\boldsymbol{z}_{m'+(n'-1)M})^H\boldsymbol{S}^H \\ &\boldsymbol{C}^{-1}\boldsymbol{s}^t_{m+(n-1)M} + (\boldsymbol{s}^t_{m+(n-1)M})^H\boldsymbol{C}^{-1}\boldsymbol{s}^t_{m'+(n'-1)M}(\boldsymbol{z}_{m'+(n'-1)M})^H\boldsymbol{S}^H \\ &\boldsymbol{C}^{-1}\boldsymbol{S}\boldsymbol{z}_{m+(n-1)M})\}. \end{aligned} \tag{102}$$

The result of (102) can be reformulated as

$$\begin{aligned}\boldsymbol{J}_{\boldsymbol{d}_r\boldsymbol{d}_r} &= 2\Re\{\sum_{m=1}^{M}\sum_{m'=1}^{M}(\overline{\lambda}_m\boldsymbol{S}^H\boldsymbol{C}^{-1}\wp_{m'} \odot (\overline{\lambda}_{m'}\boldsymbol{S}^H\boldsymbol{C}^{-1}\wp_m)^\dagger \\ &+ (\wp_m)^H\boldsymbol{C}^{-1}\wp_{m'} \odot (\overline{\lambda}_{m'}\boldsymbol{S}^H\boldsymbol{C}^{-1}\boldsymbol{S}(\overline{\lambda}_m)^H)^\dagger)\}, \end{aligned} \tag{103}$$

where $\overline{\lambda}_m = (\boldsymbol{z}_m, \cdots, \boldsymbol{z}_{m+(N-1)M})^H$, $\wp_m = (s^r_m, \cdots, s^r_{m+(N-1)M})$. Similarly, we can obtain

$$\begin{aligned}\boldsymbol{J}_{\boldsymbol{d}_r\boldsymbol{\tau}} &= 2\Re\{\sum_{m=1}^{M}(\overline{\lambda}_m\boldsymbol{S}^H\boldsymbol{C}^{-1}\boldsymbol{S}^{\boldsymbol{\tau}} \odot (\boldsymbol{R}\boldsymbol{S}^H\boldsymbol{C}^{-1}\wp_m)^\dagger \\ &+ (\wp_m)^H\boldsymbol{C}^{-1}\boldsymbol{S}^{\boldsymbol{\tau}} \odot (\boldsymbol{R}\boldsymbol{S}^H\boldsymbol{C}^{-1}\boldsymbol{S}(\overline{\lambda}_m)^H)^\dagger)\} \end{aligned} \tag{104}$$

$$\begin{aligned}\boldsymbol{J}_{\boldsymbol{d}_r\boldsymbol{f}} &= 2\Re\{\sum_{m=1}^{M}(\overline{\lambda}_m\boldsymbol{S}^H\boldsymbol{C}^{-1}\boldsymbol{S}^{\boldsymbol{f}} \odot (\boldsymbol{R}\boldsymbol{S}^H\boldsymbol{C}^{-1}\wp_m)^\dagger \\ &+ (\wp_m)^H\boldsymbol{C}^{-1}\boldsymbol{S}^{f} \odot (\boldsymbol{R}\boldsymbol{S}^H\boldsymbol{C}^{-1}\boldsymbol{S}(\overline{\lambda}_m)^H)^\dagger)\}, \end{aligned} \tag{105}$$

$$\begin{aligned}\boldsymbol{J}_{\boldsymbol{d}_r\boldsymbol{d}_t} &= 2\Re\{\sum_{m=1}^{M}\sum_{n=1}^{N}(\overline{\lambda}_m\boldsymbol{S}^H\boldsymbol{C}^{-1}\Im_n \odot (\aleph_n\boldsymbol{S}^H\boldsymbol{C}^{-1}\wp_m)^\dagger \\ &+ (\wp_m)^H\boldsymbol{C}^{-1}\Im_n \odot (\aleph_n\boldsymbol{S}^H\boldsymbol{C}^{-1}\boldsymbol{S}(\overline{\lambda}_m)^H)^\dagger)\} \end{aligned} \tag{106}$$

References

[1] T. Aittomaki and V. Koivunen, "MIMO radar filterbank design for interference mitigation," *Proceedings of 2014 IEEE International Conference on Acoustics, Speech and Signal Processing (ICASSP)* , pp.5297-5301, May 2014.

[2] P. Wang, H. Li, and B. Himed, "A parametric moving target detector for distributed MIMO radar in non-homogeneous environment," *IEEE Transactions on Signal Processing*, vol. 61, no. 9, pp. 2282–2294, May 2013.

[3] Y. Yu, A. Petropulu, and H.V. Poor, "CSSF MIMO Radar: Compressive-sensing and step-frequency based MIMO radar," *IEEE Transactions on Aerospace and Electronic Systems*, vol. 48, no. 2, pp. 1490–1504, Apr 2012.

[4] M. Rossi, A. Haimovich, and Y. Eldar, "Spatial compressive sensing in MIMO radar with random arrays," *in Proceedings of 46th Annual Conference on Information Sciences and Systems (CISS)*, pp. 1-6, Mar 2012.

[5] X. Song, P. Willett, S. Zhou, and P. Luh, "The MIMO Radar and Jammer Games," *IEEE Transactions on Signal Processing*, vol. 60, no. 2, pp. 687–699, Feb 2012.

[6] Y. Zhang, M. Amin, and B. Himed, "Joint DOD/DOA estimation in MIMO radar exploiting time-frequency representations," *EURASIP Journal on Advances in Signal Processing, Special issue on Advanced in Time-Frequency and Array Processing of Nonstationary Signals*, vol. 2012, no. 1, 2012.

[7] H. Godrich, A. Petropulu, and H.V. Poor, "Power allocation strategies for target localization in distributed multiple-radar architectures," *IEEE Transactions on Signal Processing*, vol. 59, no. 7, pp. 3226–3240 , Jul 2011.

[8] J. Li and P. Stoica, "MIMO radar with collocated antennas," *IEEE Signal Processing Magazine*, vol. 24, no. 5, pp. 106–114, Sep 2007.

[9] P. Howland, D. Maksimiuk, and G. Reitsma, "FM radio based bistatic radar," *in Proc. Inst. Elect. Eng., Radar Sonar Navig.*, vol. 152, no. 3, pp. 107C115, Jun. 2005.

[10] M. Glende, J. Heckenbach, H. Kuschel, S. Muller, J. Schell, and C. Schumacher, "Experimental passive radar systems using digital illuminators (DAB/DVB-T)," *in Proc. Int. Radar Symp. (IRS)*, Cologne, Germany, 2007, pp. 5C7.

[11] H. Griffiths, C. Baker, J. Baubert, N. Kitchen, and M. Treagust, "Bistatic radar using satellite-borne illuminators," *in Proc. RADAR*, pp. 1C5, Oct. 2002.

[12] H. Guo, K. Woodbridge, and C. Baker, "Evaluation of WIFI beacon transmissions for wireless based passive radar," *in Proc. IEEE Radar Conf. RADAR*, pp. 1C6, 2008.

[13] D. Tan, H. Sun, Y. Lu, M. Lesturgie, and H. Chan, "Passive radar using global system for mobile communication signal:theory, implementation and measurements," *Radar, Sonar and Navigation,IEE Proceedings* -, vol. 152, no. 3, pp. 116-123, June 2005.

[14] H. Griffiths and C. Baker, "Passive coherent location radar systems. Part 1: performance prediction," *Radar, Sonar and Navigation,IEE Proceedings* -, vol. 152, no. 3, pp. 153-159, June 2005.

[15] H. Griffiths and C. Baker, "Measurement and analysis of ambiguity functions of passive radar transmissions," *in Radar Conference, 2005 IEEE International*, May 2005, pp. 321-325.
[16] D. Hack, L. Patton, B. Himed, and M. Saville "Detection in passive MIMO radar networks," *IEEE Transactions on Signal Processing*, vol.62, no. 11, pp. 2999-3012, June 1, 2014.
[17] P. Stoica, E. Larsson, and A. Gershman, "The stochastic CRB for array processing:a textbook derivation," *IEEE Signal Processing Letters*, vol. 8, no. 5, pp. 148-150, May 2001.
[18] A. Dogandzic and A. Nehorai, "Cramer-Rao bounds for estimating range, velocity,and direction with a senor array," *IEEE Transactions on Signal Processing*, vol. 49, no. 6, pp. 1122-1137, June 2001.
[19] K. Rambach and B. Yang, "Colacated MIMO radar: Cramer-Rao bound and optimal time division multiplexing for DOA estimation of moving targets," *ICASSP 2013*, pp. 4006-4010
[20] M. Greco, P. Stinco, F. Gini, and A. Farina, "Cramer-Rao bounds and selection of bistatic channels for multistatic radar systems," *Aerospace and Electronic Systems, IEEE Transactionson*, vol. 47, no. 4, pp. 2934-2948, 2011.
[21] F. Gini and R. Reggiannini, "On the use of Cramer-Rao-Like bounds in the presence of random nuisance parameters," *IEEE Transactions On Communication*, vol. 48, no. 12, December 2000.
[22] R. Miller and C. Chang, "A modified Cramer-Rao bound and its applications," *IEEE Trans. Inform. Theory*, vol. 1T-24, pp. 398-400, May 1978.
[23] M. Radmard, S. Karbasi, and M. Nayebi, "Data fusion in MIMO DVB-T-Based passive coherent location," *IEEE Transactions on aerospace and electronic systems* vol. 49, no. 3 July 2013.
[24] Q. He, R. Blum, and A. Haimovich, "Noncoherent MIMO Radar for location and velocity estimation: more antennas means better performance," *Signal Processing. IEEE Transactions on*, vol. 58, no. 7, pp. 3661-3680, July 2010.
[25] P. Stinco, M. Greco, F. Gini, and M. Rangaswamy, "Ambiguity function and Cramer-Rao bounds for universal mobile telecommunications system-based passive coherent location systems," *IET Radar, Sonar and Navigation*, vol. 6, no. 7, pp. 668-678, 2012.
[26] Q. He and R. Blum, "The significant gains from optimally processed multiole signals of opportunity and multiple receive stations in passive radar," *IEEE Signal Processing Letters*, vol. 21, no. 2, pp. 180-184, February 2014.
[27] S. Gogineni, M. Rangaswamy, B. Rigling, and A. Nehorai, "Cramr-Rao bounds for UMTS-Based passive multistatic radar," *IEEE Transactions on Signal Processing*, vol. 62, no. 1, pp. 95-106, January 1,2014.
[28] M. Skolnik, "Radar handbook, third edition," February 12, 2008.
[29] S. Kay, "Fundamentals of Statistical Signal Processing: Estimation Theory," *Prentice-Hall. Englewood Cliffs*, NJ, 1993.
[30] K. Petersen and M. Pedersen, "The matrix cookbook," http://matrixcookbook.com, version: 2012.11.15.
[31] C. Fritsche, U. Orguner, E. Ozkan, F. Gustafsson, "On the Cramer-Rao lower bound under model mismatch," ICASSP 2015.